Supporting Info

Carbohydrates@MOFs

Efwita Astria[1‡], Martin Thonhofer[1,2‡], Raffaele Ricco[1], Weibin Liang[3], Angela Chemelli[4], Andrew Tarzia[3], Karen Alt[5], Christoph E. Hagemeyer[5], Johannes Rattenberger[6], Hartmuth Schroettner[6], Tanja Wrodnigg[7], Heinz Amenitsch[4], David M. Huang[3], Christian J. Doonan[3]*, Paolo Falcaro[1,3]*

1) Institute of Physical and Theoretical Chemistry, Graz University of Technology, 8010 Graz, Austria 2) Laboratory for Characterisation and Processing of Polymer, Faculty of Mechanical Engineering, University of Maribor, SI-2000, Maribor, Slovenia 3) Department of Chemistry, The University of Adelaide, 5005 Adelaide, South Australia 4) Institute of Inorganic Chemistry, Graz University of Technology, 8010 Graz, Austria 5) Australian Centre for Blood Diseases, Monash University, Melbourne, Australia 6) Graz Centre for Electron Microscopy (ZFE), 8010 Graz, Austria 7) Institute of Organic Chemistry, Graz University of Technology, 8010 Graz, Austria.

CONTENTS:

Experimental Section

Materials

D-glucose (**1**), D-mannose (**2**), D-galactose (**3**), D-xylose (**4**), methyl-β-D-glucopyranoside, (**5**) D-glucitol (**6**), meglumine (**7**), *N*-acetyl-D-glucosamine (**8**), D-glucosamine hydrochloride (**9**), sucrose (**10**), maltodextrin (**11**, approximately 20 α-1,4-D-glucose units), ethylene glycol (**12**) and *N*-methyl-aminoethanol (**13**), Carboxymethyl dextran (**CM-dextran**, average Mol. Wt: 10.000-20.000), FITC-tagged carboxymethyl dextran (**FITC-CM-dextran**, average Mol. Wt: 40.000, 1-8 mmol FITC/mol glucose, carboxymethyl groups content: 3-7%), and EDTA disodium salt were purchased from Sigma-Aldrich. Zinc acetate dihydrate (**$Zn(OAc)_2{\cdot}2H_2O$**) was purchased from Merck Millipore. 2-Methylimidazole (**2mIM**) was purchased from TCI chemicals. MOFs growth on paper was performed using 589^3 Blue ribbon S&S Filter paper circles (Ø = 110 mm). All solutions were prepared in deionized water (DI Water). Absolute ethanol for washings was purchased from Fisher Scientific and used without further purification. Unless otherwise specified, all reactions were conducted into 2mL plastic Eppendorf vials.

General procedure for the preparation of monosaccharides@ZIF-8

In 20 mL glass vials, compounds **1-13** were dissolved in 5 mL of aqueous solutions of 2mIM (initial concentration: 160 mM) to provide different sugar concentrations ranging from 0.01 M to 1 M. After 30 min, 5 mL of aqueous solutions of $Zn(OAc)_2{\cdot}2H_2O$ (initial concentration: 40 mM) were added at once, and the reaction mixtures left to stir at room temperature on a tube rotator at 20 rpm. After 12 h, 20 mL of EtOH were added dropwise (within 15 min), and the reaction mixtures rotated for additional 8 h. The formed particles were concentrated by centrifugation (5750 rcf, 7 minutes) and washed with water (3x 7 mL) and EtOH (3x 7 mL) respectively. The resulting white powders were dried for 24 h at ambient pressure and temperature.

Attempted synthesis of dextrans@ZIF-8

The solution of 2mIM (initial concentration 160 mM) was mixed with dextran sugars in 1 mL DI water. The separate solution of $Zn(OAc)_2{\cdot}2H_2O$ (initial concentration: 40 mM, 1 mL) was also prepared. The two solutions were mixed and left at room temperature for 24 hours without stirring. Details on the substrates used are reported in Supporting Table S4

Growth @ZIF-8 on glass and paper substrates

The aqueous solution of 2mIM (initial concentration: 160 mM, 6 mL) was mixed with $Zn(OAc)_2{\cdot}2H_2O$ (initial concentration: 40 mM, 6 mL), a glass plate (vial **a**), CM-dextran 0.36 mg/mL (vial **b**) and a piece of paper (589^3 Blue ribbon S&S Filter paper circles 110 mm) (vial **c**). The video screenshots were taken at 30 second, 30 minutes and 24 hours.

Synthesis of CM-dextran@ZIF-8 (CM@ZIF-8) with different ligand/metal ratios

CM@ZIF-8 samples were synthesized by mixing aqueous stock solutions of 2mIM (initial concentration: 3.84 M) and CM-dextran (final amount: 0.36 mg/mL), adding water when necessary, according to the different final ratios of ligand and metal chosen ($2mIM/Zn^{2+}$ = 2.52, 3.47, 4, 6, 8, 16). The solutions were stirred in vortex mixer for three seconds. Subsequently, a stock solution of $Zn(OAc)_2{\cdot}2H_2O$ (initial

concentration: 0.24 M) was added. Total final volume for each sample was 2 mL. The solutions were briefly vortex-mixed (three seconds) and left standing at room temperature (no stirring) for 24 hours. The precipitates were collected by centrifugation (9660 rcf, 5 min), washed with DI water (3x), ethanol (3x). The resulting white powders were dried for 24 h at ambient pressure and temperature.

Synthesis of CM@ZIF-8 "B series"

Samples with the ratio Zn^{2+}:2mIM = 1:3.47 were prepared by mixing $Zn(OAc)_2 \cdot 2H_2O$ solution (initial concentration: 105.5 mM, 1 mL) with 2mIM aqueous solution (initial concentration: 30.4 mM, 1 mL) and CM-dextran solutions (Final amount: 0.36 mg/mL reaching final amounts as follows: B1 = 0.18, B2 = 0.36, B3 = 0.72, B4 = 1.44 mg/mL). Total final volume for each sample was 2 mL. The solutions were briefly vortex-mixed (three seconds) and left standing at room temperature (no stirring) for 24 hours. The precipitates were collected by centrifugation (9660 rcf, 5 min), washed with DI water (3x), ethanol (3x). The resulting white powders were dried for 24 h at ambient pressure and temperature.

Synthesis of FITC-CM-dextran@ZIF-8 (FITC-CM@ZIF-8) "BF series"

Synthesis of FITC-CM@ZIF-8 was analogous to synthesis of CM@ZIF-8 "B series", but using FITC-CM-dextran in place of CM-dextran, and under the same conditions. Total final volume for each sample was 2 mL. The solutions were briefly vortex-mixed (three seconds) and left standing at room temperature (no stirring) for 24 hours. The precipitates were collected by centrifugation (9660 rcf, 5 min), washed with DI water (3x), ethanol (3x) and used for the further release tests.

Washing Procedure Optimization

A suspension of ZIF-8 (3.4 mg/mL, 45 mL) was mixed with CM-dextran solution (36 mg/mL, 3 mL), and left at room temperature for 1 hour. 2 mL aliquots were taken and washed with water (1x, or 3x) or ethanol (3x). An additional aliquot of 30 mL was equally divided into 3 vials, and each of them was consecutively washed with water, and ethanol, and the solid residuals immersed in SDS (0.1%, 1% and 10%, respectively) for 30 minutes. After centrifugation, the supernatants were removed and the precipitates were washed 2x with MOPS (3-(*N*-morpholino)propanesulfonic acid) buffer (10 mM, pH = 7.4), and 2x with ethanol (see **Figure S42**).

Release tests of FITC-CM@ZIF-8 "BF2 sample" by different amounts of EDTA

BF2 samples were washed 3X with DI Water then mixed with 600 µL DI water. For each BF2 samples, 600 µL EDTA solution (initial concentrations: 20, 40, 80 mM) was added afterwards. The sample was vortex-mixed for three seconds. At regular intervals of 1 hour, the mixture was centrifuged (11337 rcf, 1 min), and 1 mL of the supernatant taken with micropipettes. The absorbance was measured by UV-VIS spectroscopy (Thermo Scientific Nano Drop One^c, λ_{max}: 490 nm).

Table S1. Tested monosaccharides.

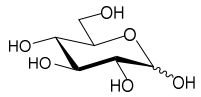	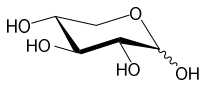	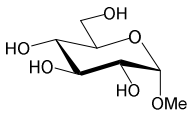	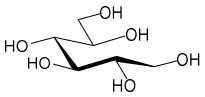
D-Glucose	D-Xylose	Methyl-α-D-glucopyranoside	D-Glucitol
1	**4**	**5**	**6**

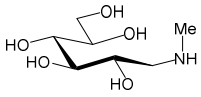	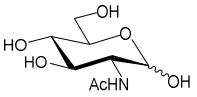	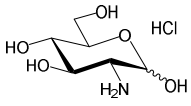	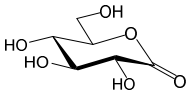
Meglumine	*N*-Acetyl-D-glucosamine	D-Glucosamine hydrochloride	D-Gluconic acid-δ-lactone
7	**8**	**9**	**11**

Table S2. Calculated amounts of the respective monosaccharides for the preparation of different concentrations in a 2mIM solution.

The concentrations of carbohydrate listed in **Table S2** are related to the 1st precursor solution (2mIM). Due to the dilution in the next step (addition of the same volume of the 2nd precursor solution ($Zn(OAc)_2$), the final concentration halves. These final, total concentrations are given in the following pictures and tables.

Compound	**1**	**4**	**5**	**6**	**7**	**8**	**9**	**11**	
M (g/mol)	180,16	150,13	194,18	182,17	195,21	221,21	215,63	178,14	
m (g)	0,4504	0,3753	0,4855	0,4554	0,4880	0,2765	0,2695	0,4454	
Vol (mL)	1	1	1	1	1	1	1	1	**A**
c (mol/L)	2,5	2,5	2,5	2,5	2,5	1,25[1)]	1,25[1)]	2,5	
m (g)	0,3603	0,3003	0,3884	0,3643	0,3904	0,4424	0,4313	0,3563	
Vol (mL)	2	2	2	2	2	2	2	2	**B**
c (mol/L)	1	1	1	1	1	1	1	1	
Vol_B (mL)	0.5	0.5	0.5	0.5	0.5	0.5	0.5	0.5	
Vol_{2mIM} (mL)	0.5	0.5	0.5	0.5	0.5	0.5	0.5	0.5	**C**
c (mol/L)	0.5	0.5	0.5	0.5	0.5	0.5	0.5	0.5	
Vol_B (mL)	0.1	0.1	0.1	0.1	0.1	0.1	0.1	0.1	
Vol_{2mIM} (mL)	0.9	0.9	0.9	0.9	0.9	0.9	0.9	0.9	**D**
c (mol/L)	0.1	0.1	0.1	0.1	0.1	0.1	0.1	0.1	
Vol_B (mL)	0.01	0.01	0.01	0.01	0.01	0.01	0.01	0.01	
Vol_{2mIM} (mL)	0.99	0.99	0.99	0.99	0.99	0.99	0.99	0.99	**E**
c (mol/L)	0.01	0.01	0.01	0.01	0.01	0.01	0.01	0.01	

Table S3. pH-values of the respective reaction mixtures.

	1	**4**	**5**	**6**	**7**	**8**	**9**	**11**	Final concentration
	D-Glucose	**D-Xylose**	**Methyl-α-D-gluco pyranoside**	**D-Glucitol**	**Meglumine**	***N*-Acetyl-D-glucosamine**	**D-glucosamine hydrochloride**	**D-Gluconic acid δ-lactone**	
A	10	10	10	10	14	10	6	1	1.250 M
B	10	10	10	10	14	10	6	2	0.500 M
C	10	10	10	10	14	10	8	3	0.250 M
D	10	10	10	10	12	10	10	8	0.050 M
E	10	10	10	10	10	10	11	10	0.005 M

The blue highlighted samples show a clear formation of precipitate after 5 min. The respective amounts were indicated visually and are indicated from dark blue (highest amount) to light blue (lowest amount).

There are different explanations on the effect of these sugars on the formation of MOF.

For substrates **1** and **4**, a possible effect would occur during the α to β anomeric mutarotation of glucose, in which the interaction between the open aldehyde intermediate and the 2-methylimidazole ligand starts to become statistically appreciable at the highest concentration studied. This also explain why the substrates **5** (blocked due to methyl group) and **6** (a polyol) does not show the same, although weak, effect.

Substrate **7** is basic due to the presence of a secondary amine, and can easily deprotonate the ligand, whereas amide substrate **8** is more basic than a normal sugar and permits deprotonation as well, although in a minor extent than 7.

Substrate **9** has similar basic activity as 7 when freebase, however here it is present in its hydrochloride form. The more HCl sugar is added, the more the ligand is protonated, whereas at the lowest concentration the residual ligand that has not been protonated by hydrochloric acid can be deprotonated by the now freed glucosamine.

Similarly, **11** as an organic acid can easily interact with 2-methylimidazole and prevent the formation of the framework, so only at the lowest concentration studied its amount has minimal effect in the ZIF reaction.

Table S4. Tested Polysaccharides.

Video A compares the biomimetic mineralization effect of different polysaccharides. In a typical experiment, 1 mg of the respective carbohydrate (listed in **Table S4**) was dissolved in 1 mL of a freshly prepared 2mIM solution (160 mM in DI water) at ambient temperature. After 30 min, the 1 mL of the 2nd precursor solution ($Zn(OAc)_2$, 40mM in DI water) was added at once.

Sample		**MW (g/mol)**	**Detail**	**Biomimetic Mineralization**
A	No polysaccharides added	-	Control sample (blank)	Control (No)
B	Maltodextrin	3.000-4.000	-	No
C	Dextran	6.000	-	No
D	Dextran	40.000	-	No
E	Dextran	70.000	-	No
F	Diethylaminoethyl dextran (DEAE-dextran)	10.000	2.5-4.5% nitrogen; (ca. one substituent on every 3rd glucose unit)	No
G	Carboxymethyl dextran sodium salt (CM-dextran)	10.000-20.000	1.1-1.5 mmol/g; (ca. one substituent on every 3rd glucose unit)	Yes

Table S5. Yield of CM-dextran@ZIF-8 B recipe.

Sample	**Actual Yield (mg)**	**Theoretical Yield (mg)**	**Yield %**
B1	0.24	7.28	3.3
B2	1.02	7.64	13.35
B3	1.14	8.36	13.64
B4	0.84	9.8	8.57

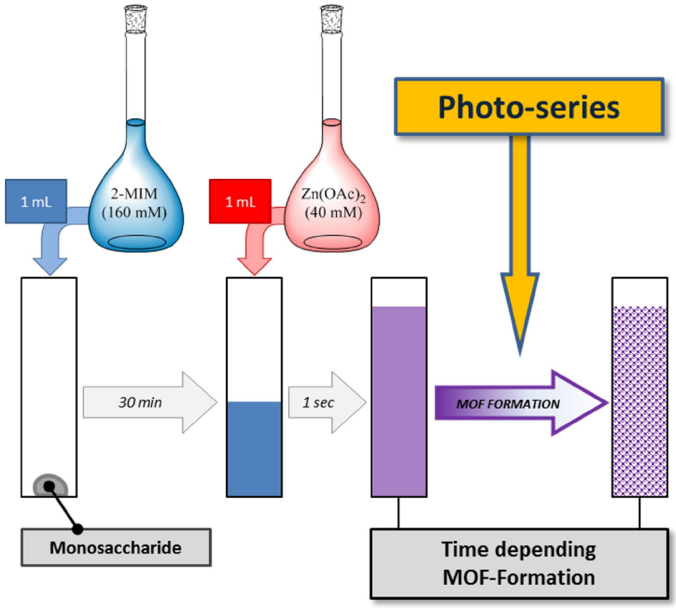

Figure S1. Schematic overview of the performed MOF-synthesis.

As indicated in **Figure S1** and according to **Table S2**, a particular amount of the respective monosaccharide (listed in **Table S1**) was dissolved in the indicated volume of a freshly prepared 2mIM solution (160 mM in DI water) at ambient temperature to provide a set of samples with different concentrations of each carbohydrate in the 1st precursor solution. Lower concentrations of the respective mixtures were achieved by diluting a particular volume the 1 M stock solution with the previously prepared 2mIM solution (160 mM in DI water) as listed in table 2. After 30 min, 1 mL of the 2nd precursor solution ($Zn(OAc)_2$, 40mM in DI Water) was added at once.

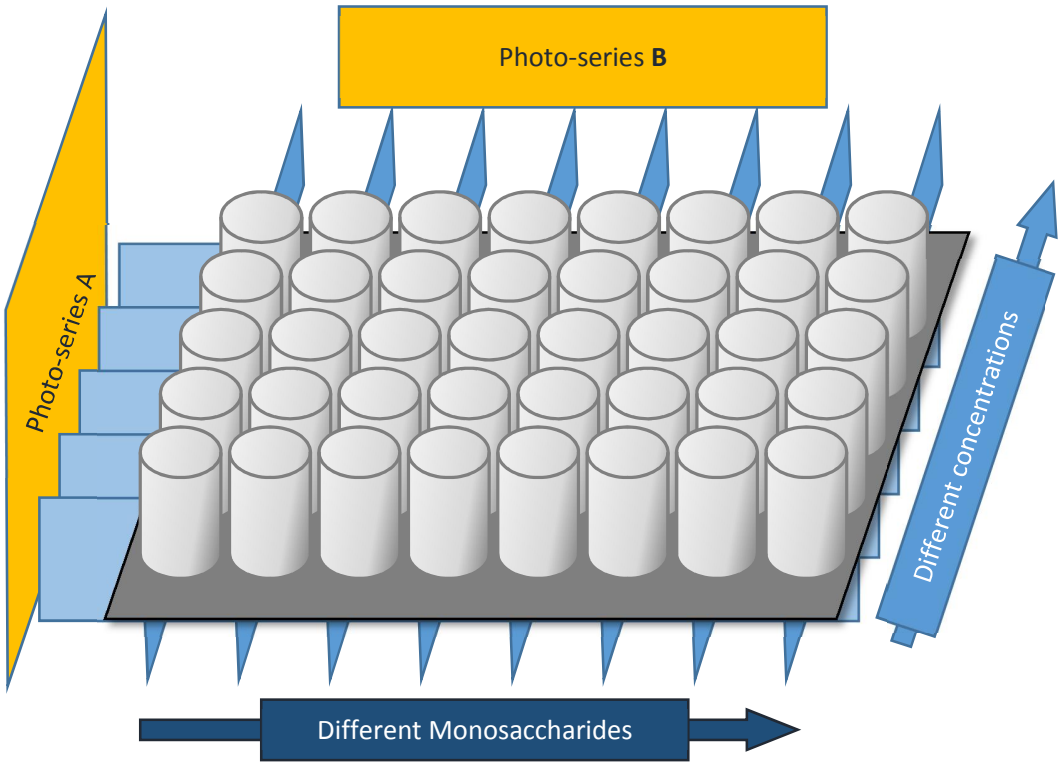

Figure S2. General schematic of the performed Photo-series.

Starting from now, time-dependent series of photos (compare **Figure S2**), comparing different carbohydrates at one concentration respectively (Photo series A) as well as each carbohydrate at different concentrations ((Photo series B), were collected. The obtained results are shown in **Figure S3-S7** and **Figure S13-S15** respectively.

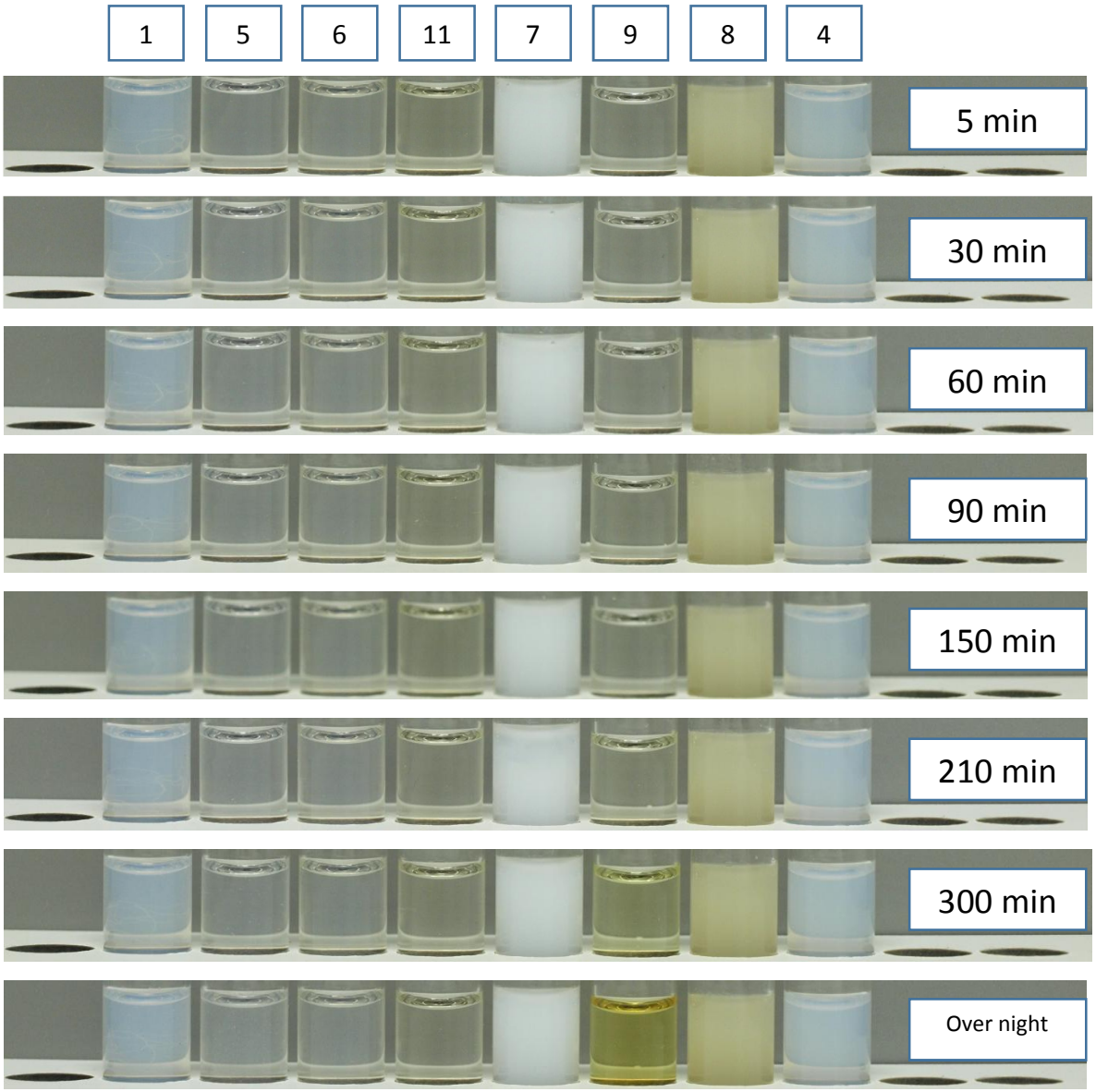

Figure S3. Time-dependent MOF formation induced by different carbohydrates (1.250 M in total).

The concentration of the corresponding monosaccharides is 1.250 M. Addition of Meglumine (**7**) clearly induces ZIF-8 formation. Although translucent solutions were obtained when with the addition of D-Glucose (**1**) and D-Xylose (**4**), it was not possible to isolate a significant amount of solid sample from a 2 mL vial. To ascertain the encapsulation of the respective carbohydrates in the final product, several vials with the same reagents were prepared (see Table S2), however the carbohydrate was never detected within the obtained solid material (see figure S3). The nitrogen containing sugars **8** and **9** show a typical colour change to yellow possibly due to various decomposition reactions, such as Amadori-rearrangements and *N*-oxide formation.[1] For $GlcNH_2$ (**9**), a solid product is not observed. We believe the reason is the presence and excess (1.25 M) of $GlcNH_2$ hydrochloride (needed in commercial samples due to the higher stability) compared to 2mIM (0.16 M), thus a basic catalysed reaction is not possible.

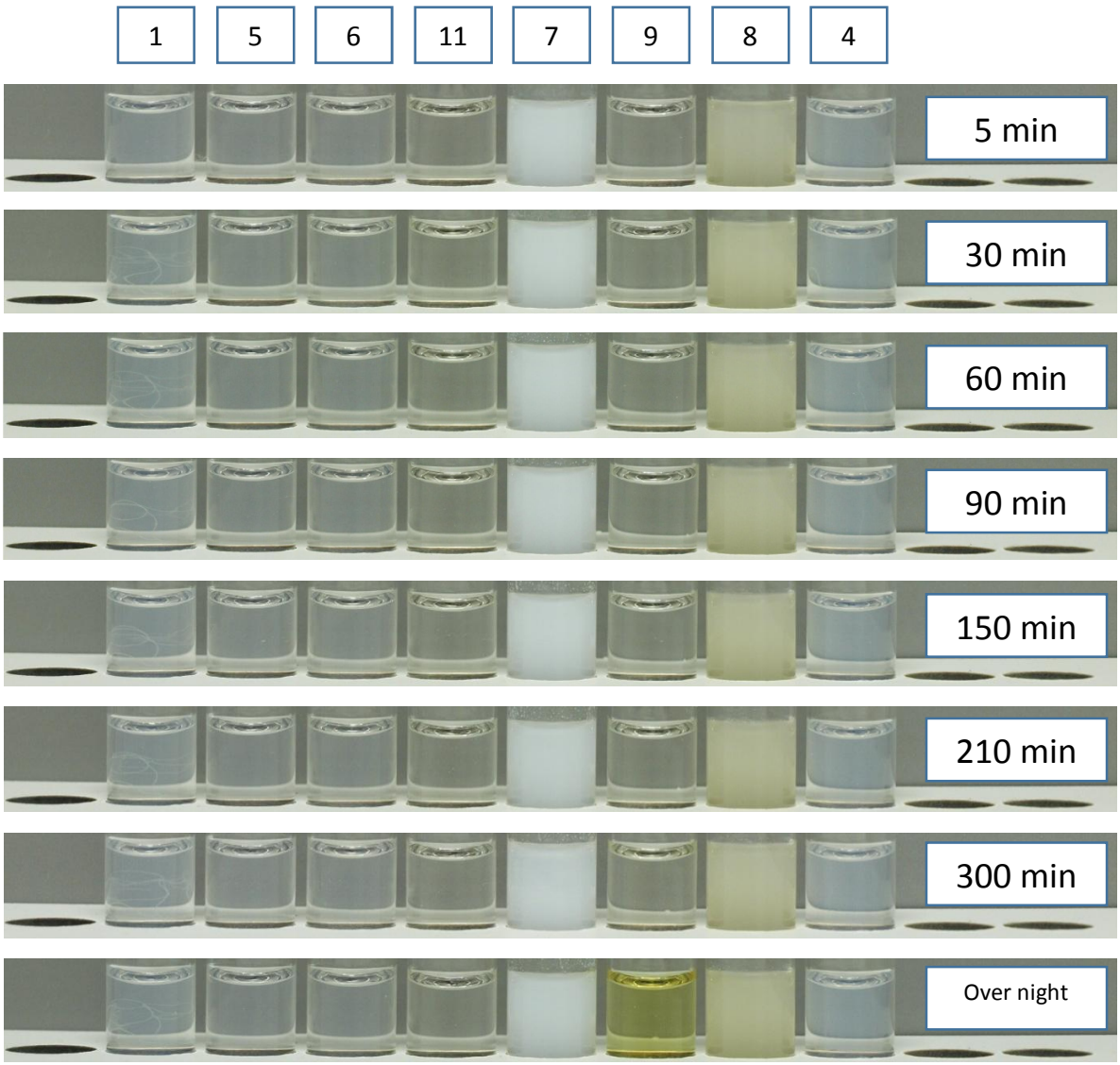

Figure S4. Time-dependent MOF formation induced by different carbohydrates (0.50 M in total).

The concentration of the corresponding monosaccharides is 0.50 M .

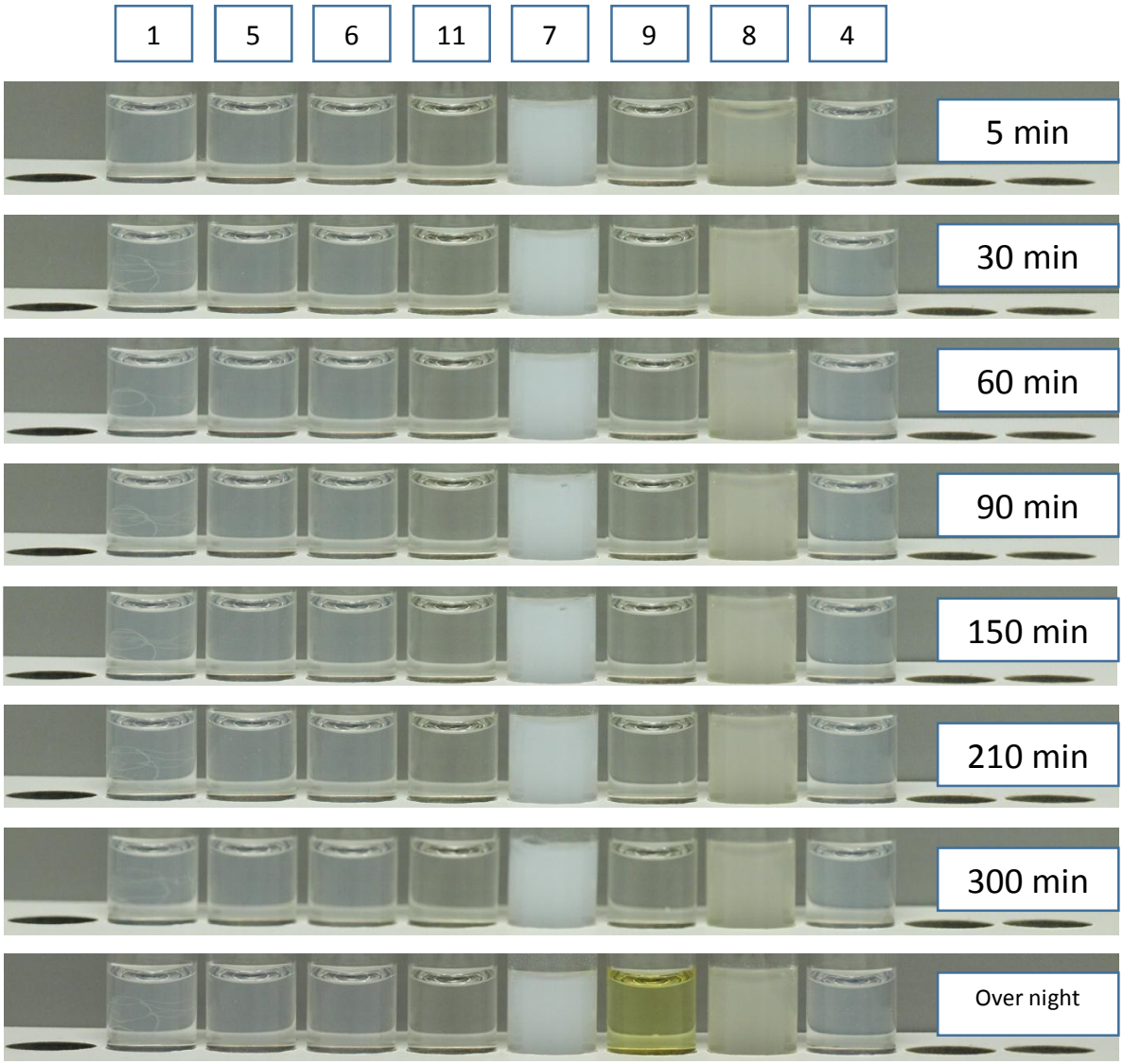

Figure S5. Time-dependent MOF formation induced by different carbohydrates (0.250 M in total).

The concentration of the corresponding monosaccharides is 0.250 M.

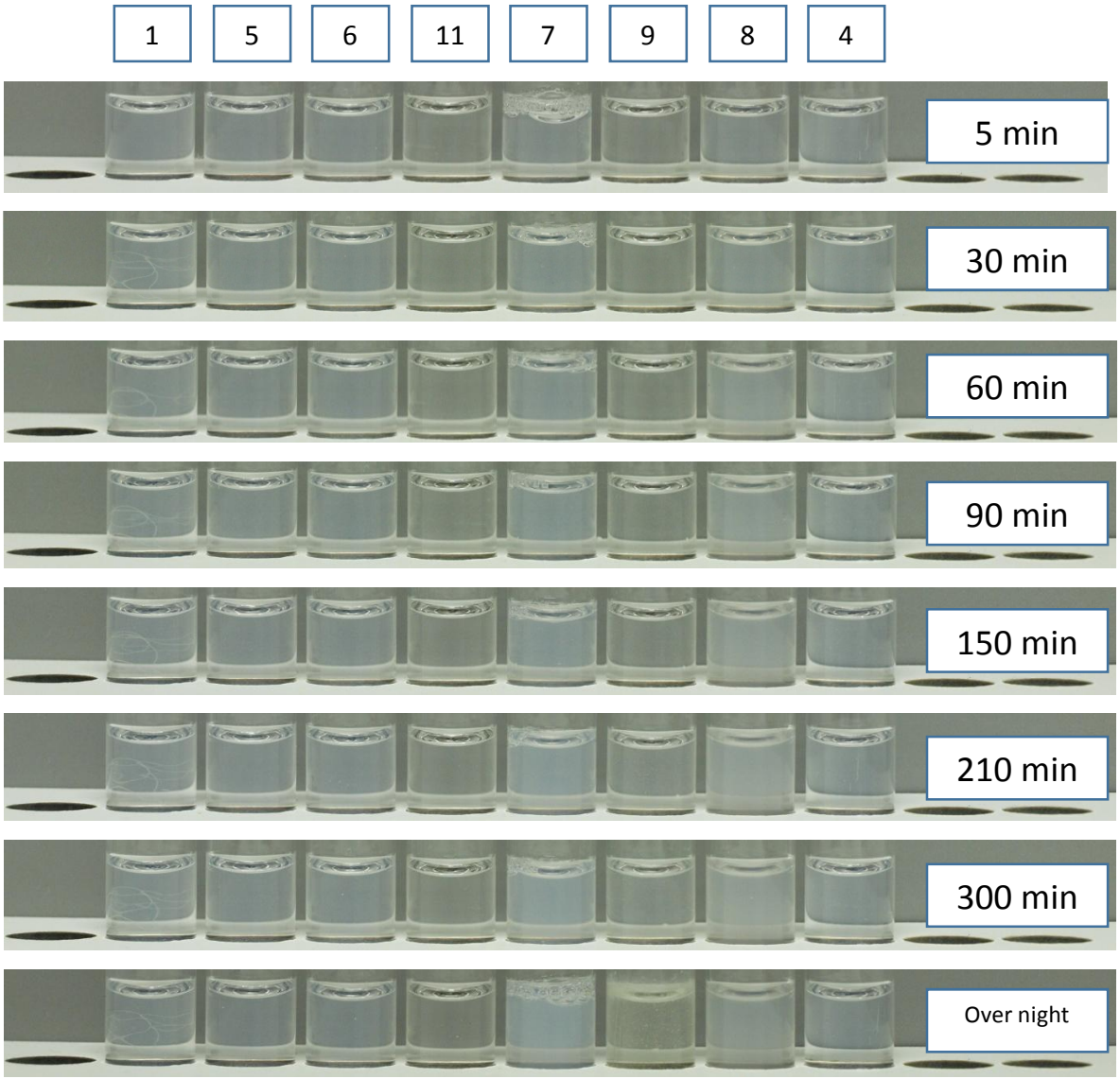

Figure S6. Time-dependent MOF formation induced by different carbohydrates (0.050 M in total).

The concentration of the corresponding monosaccharides is 0.050 M

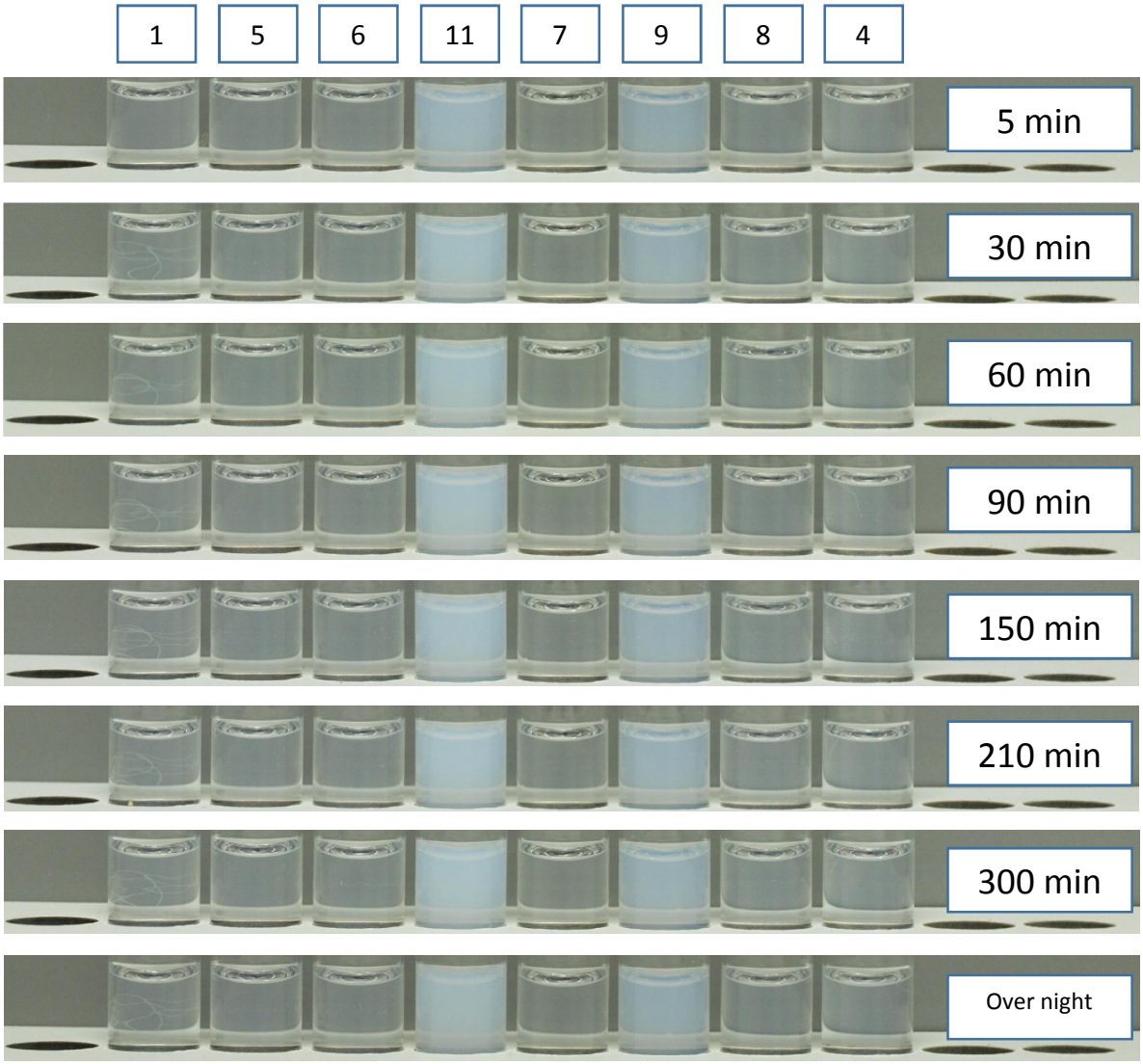

Figure S7. Time-dependent MOF formation induced by different carbohydrates (0.005 M in total).

The concentration of the corresponding monosaccharides is 0.005 M. With this concentration, $GlcNH_2$ (**9**) seems to trigger the formation of MOF particles. We think the low concentration of $GlcNH_2$ hydrochloride (0.005 M) compared to 2mIM (0.16 M) could play a role, HCl is neutralized by 2mIM and due to the liberated amino functionality the known basic catalysed reaction occurs (deprotonation of 2mIM). The same effect is observed in the sample with D-gluconic acid-δ-lactone (**11**) which might be related to the equilibrium between the lactone, carboxylic acid and carboxylate of the carbohydrate.

These hypothesis are further supported by the measured pH-values of the respective samples (see **Table S3**).

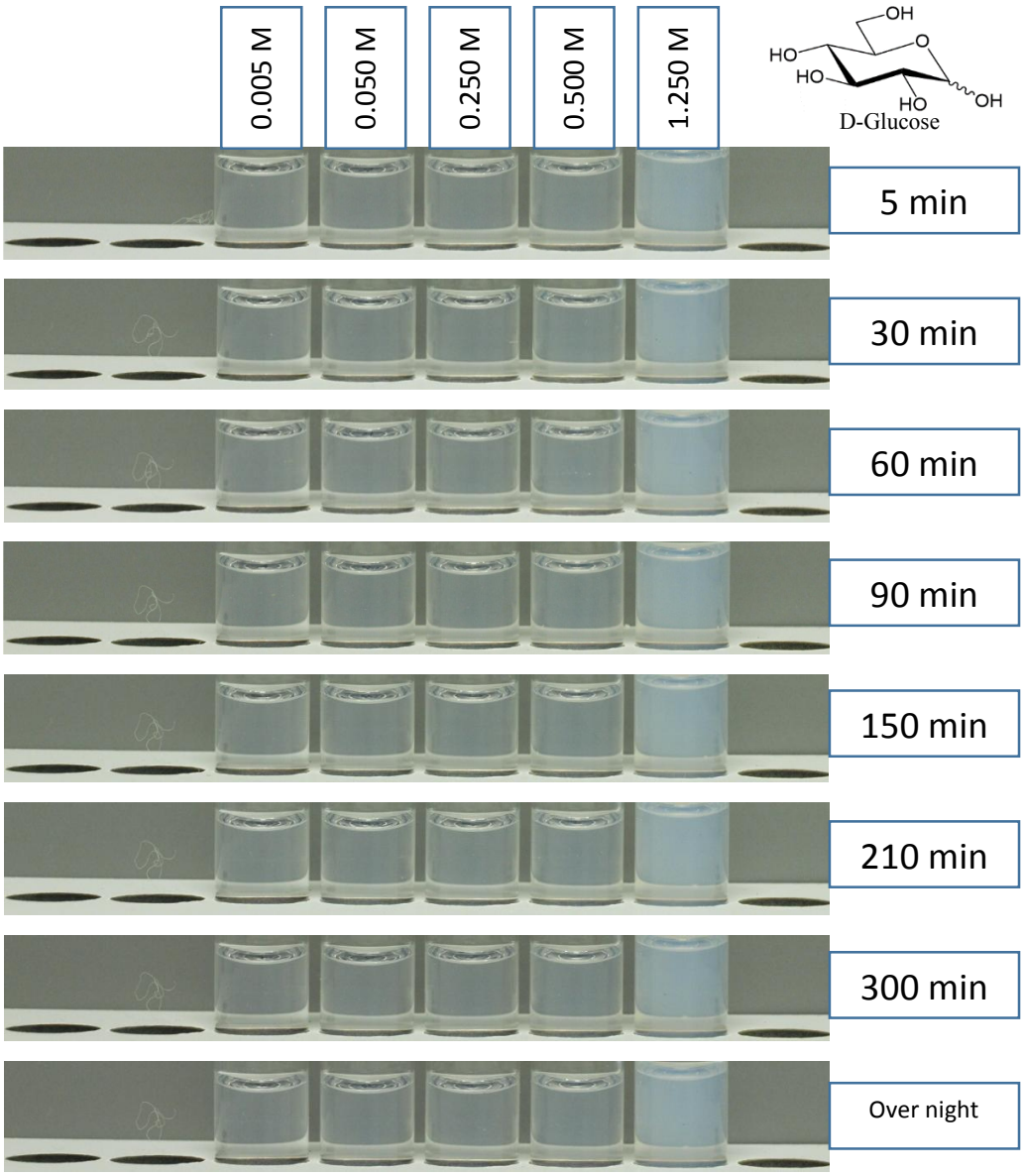

Figure S8. Time-dependent MOF formation induced by different concentrations of D-Glucose (**1**) at different concentrations.

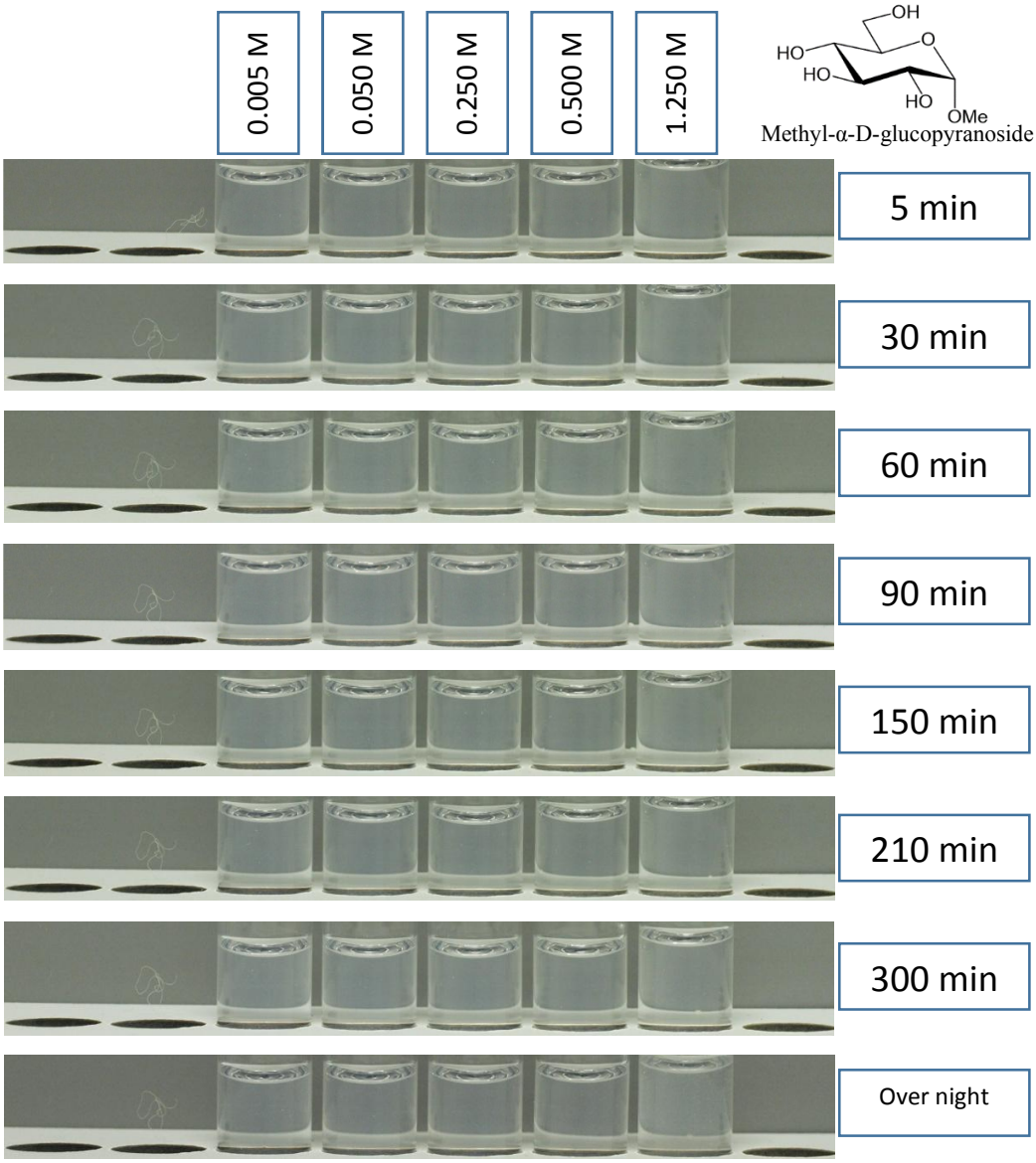

Figure S9. Time-dependent MOF formation induced by different concentrations of Methyl α-D-Glucopyranoside (**5**) at different concentrations.

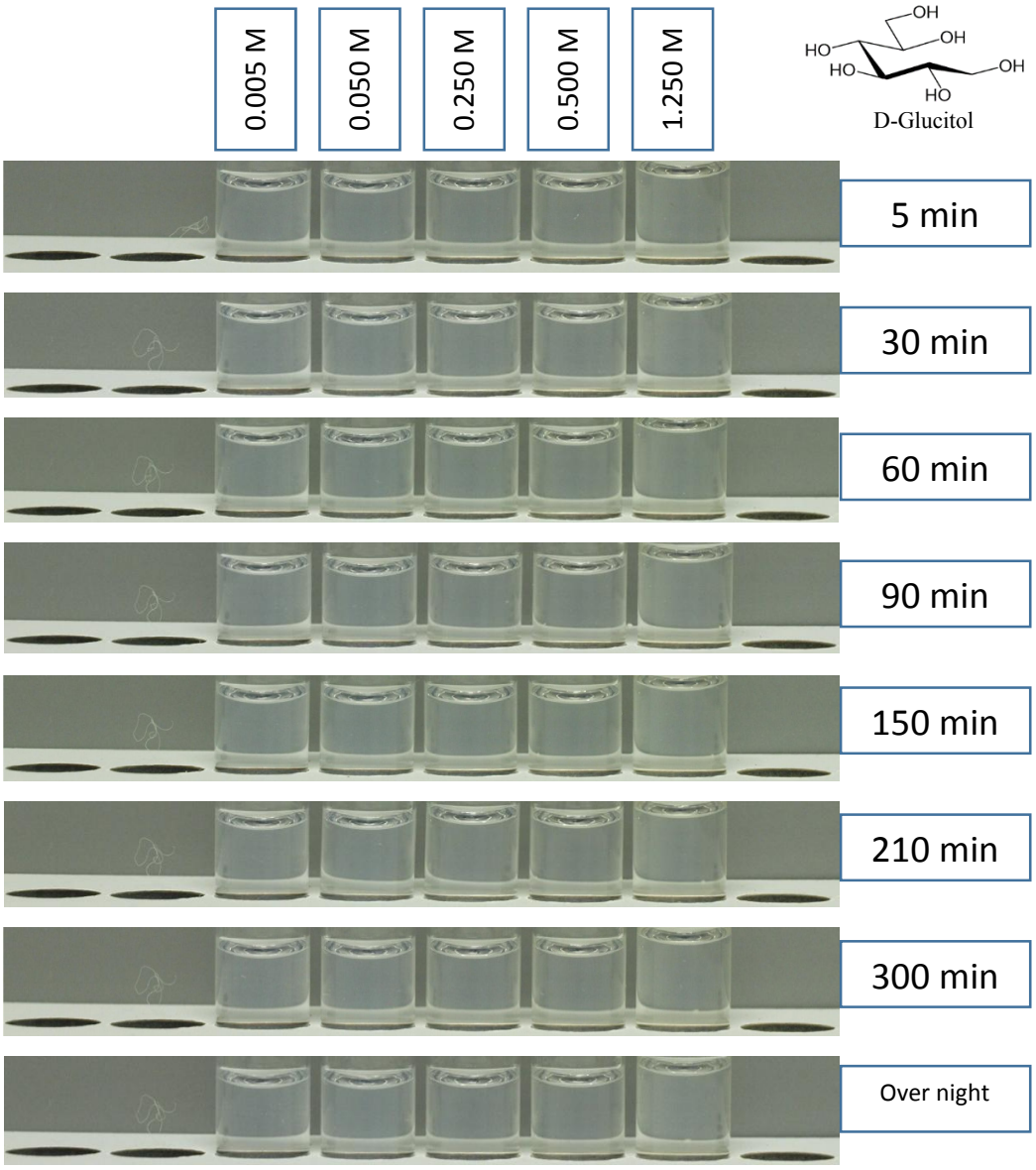

Figure S10. Time-dependent MOF formation induced by different concentrations of D-Glucitol (**6**) at different concentrations.

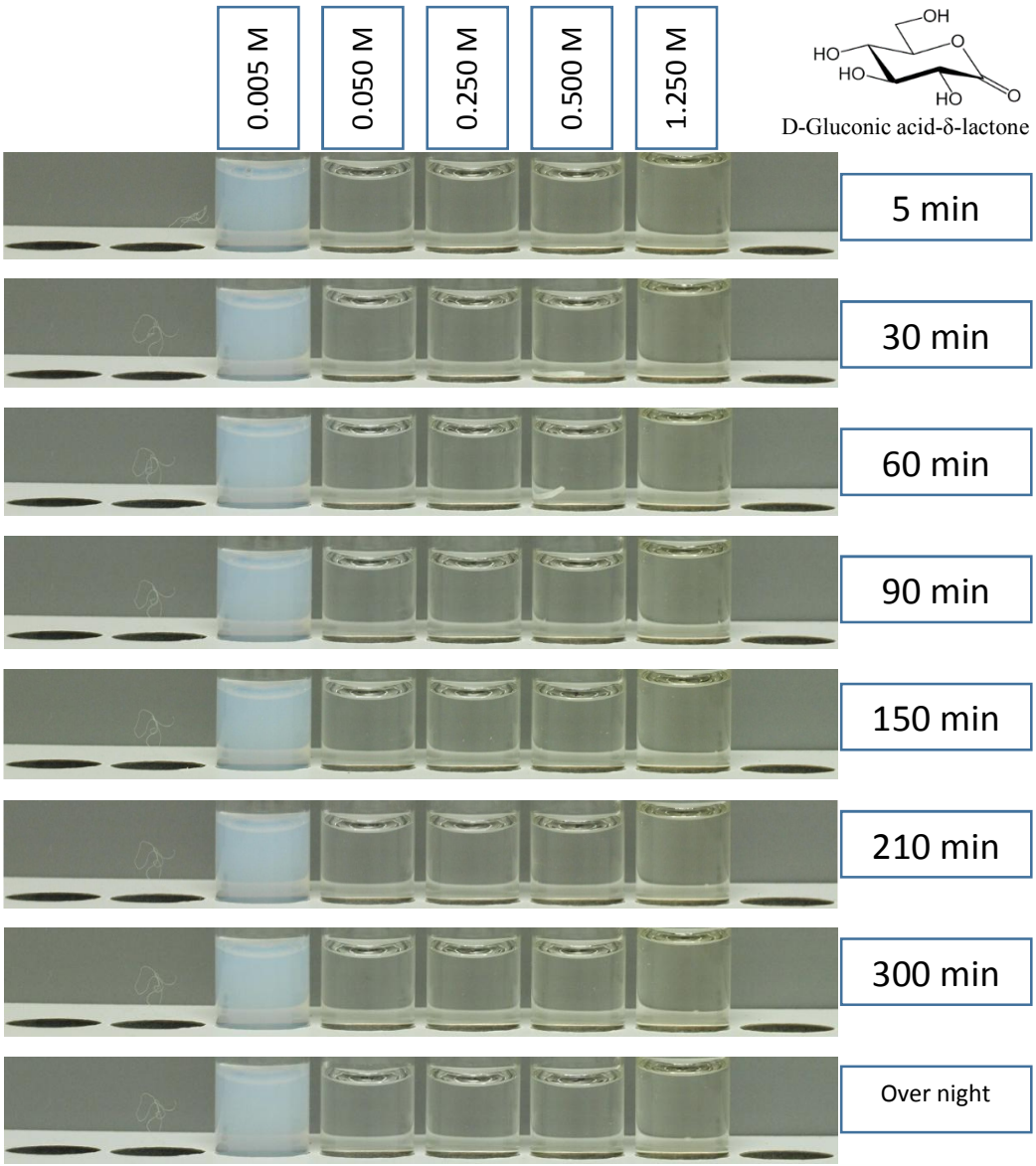

Figure S11. Time-dependent MOF formation induced by different concentrations of D-Gluconic acid-δ-lactone (**11**) at different concentrations.

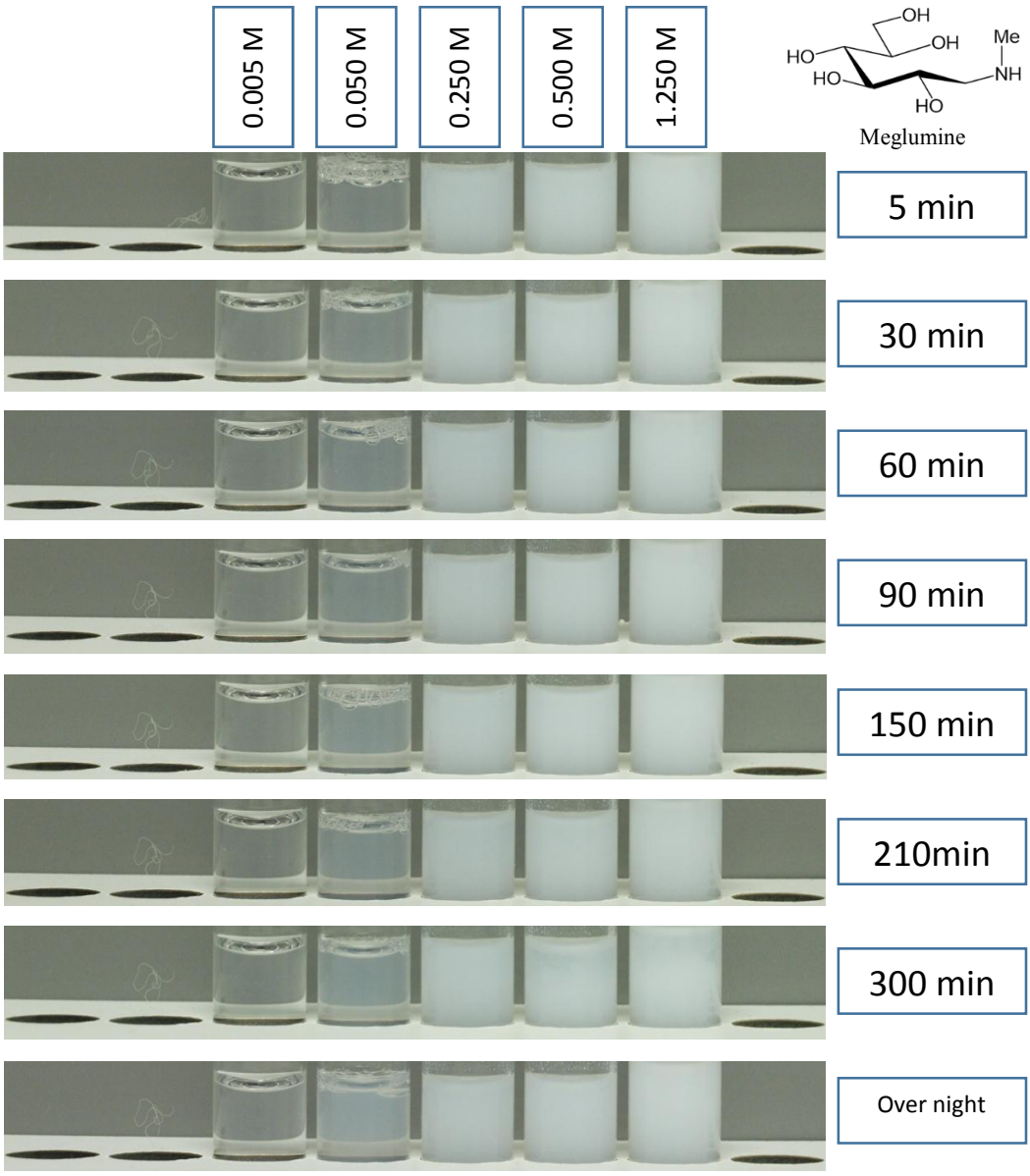

Figure S12. Time-dependent MOF formation induced by different concentrations of Meglumine (**7**) at different concentrations.

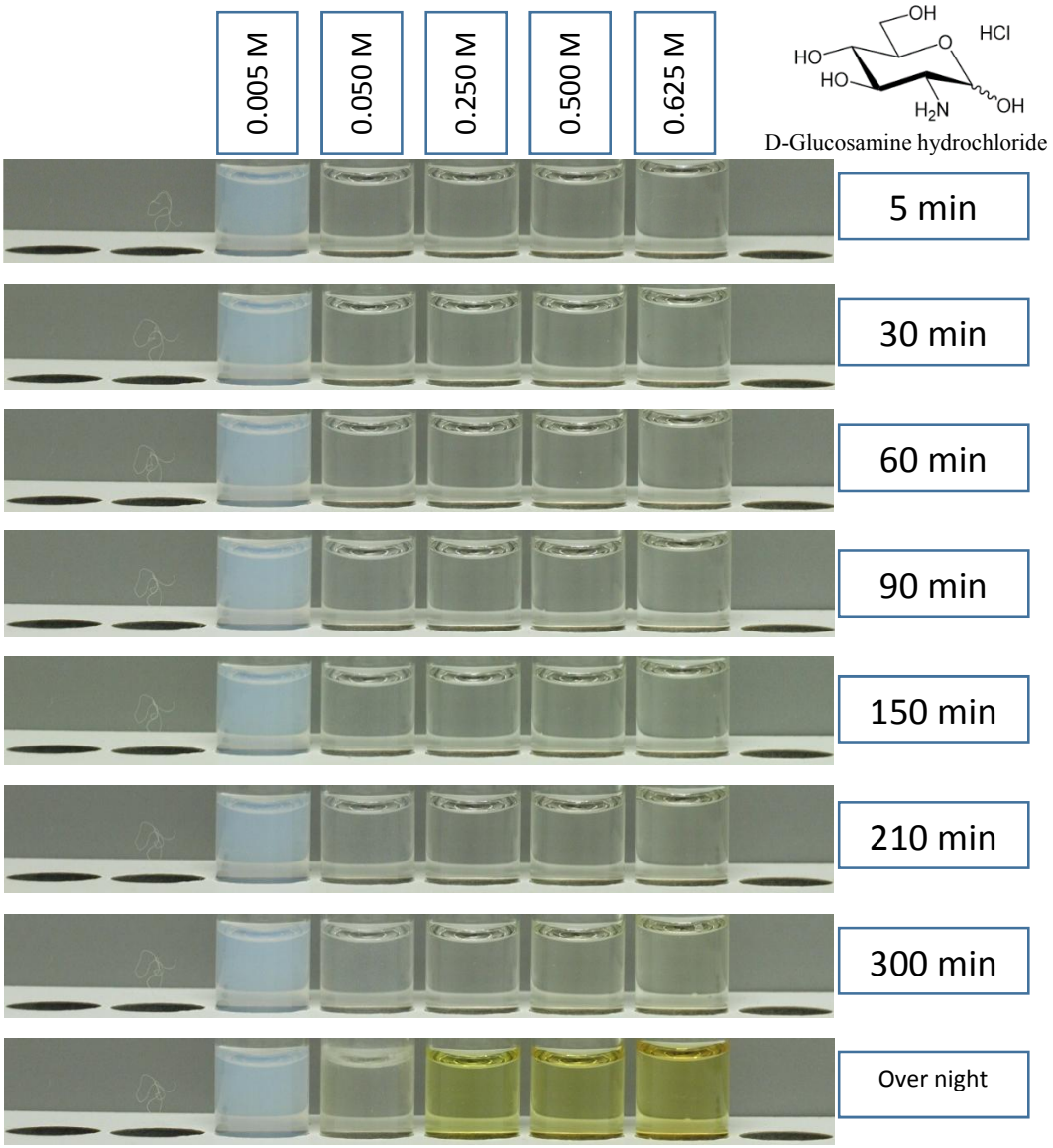

Figure S13. Time-dependent MOF formation induced by different concentrations of D-Glucosamine HCl (**9**) at different concentrations.

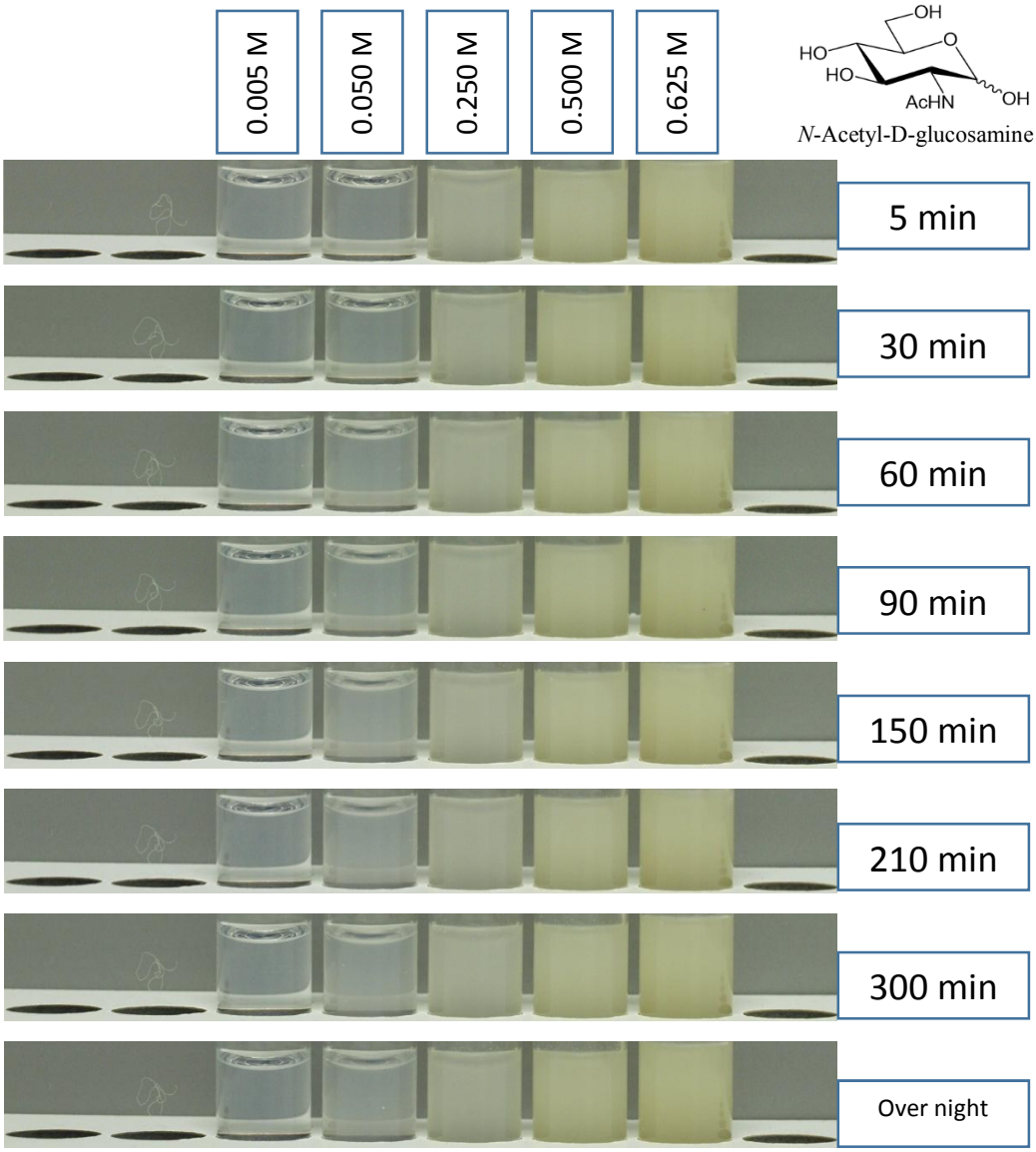

Figure S14. Time-dependent MOF formation induced by different concentrations of *N*-Acetyl-D-glucosamine (**8**) at different concentrations.

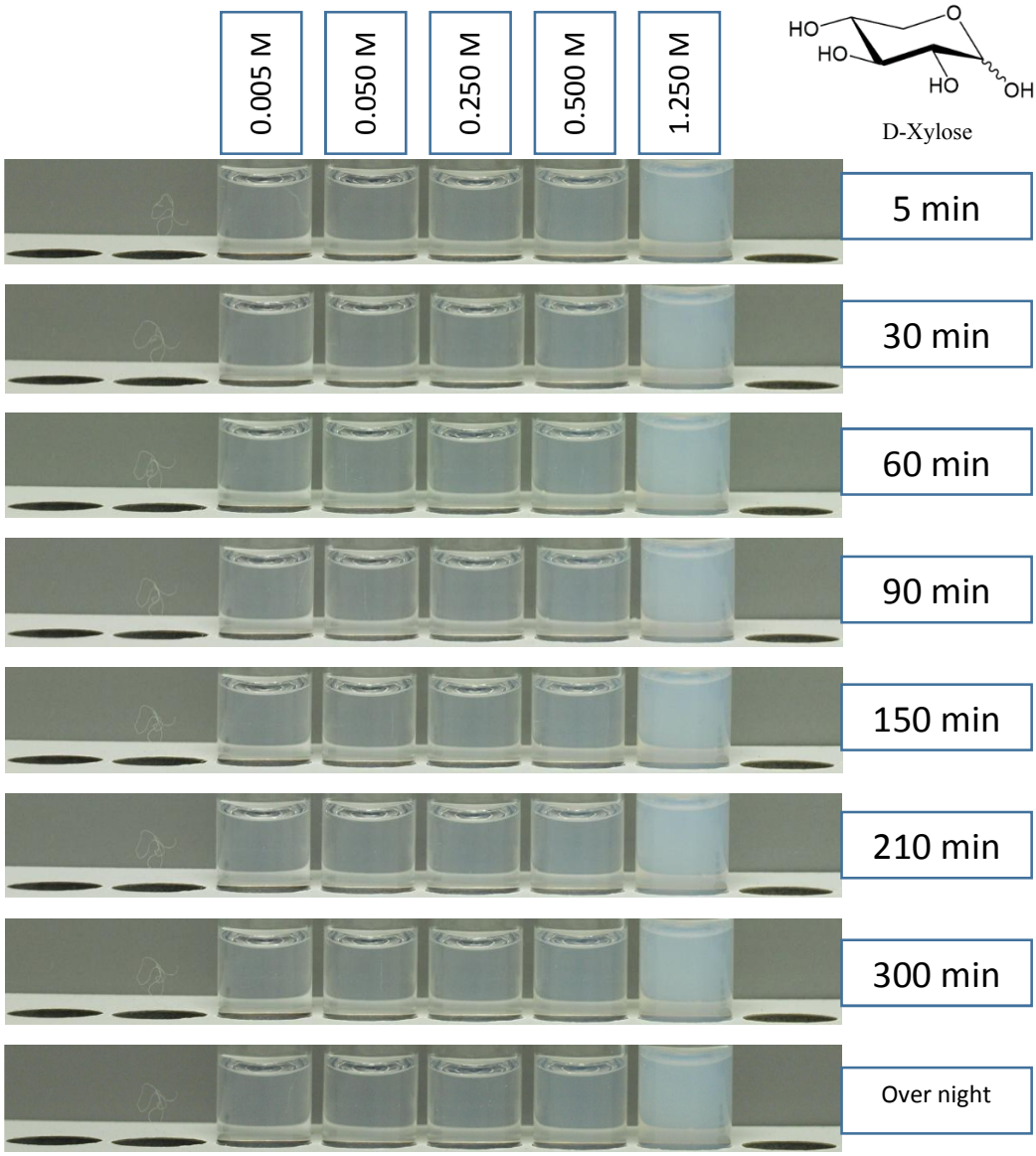

Figure S15. Time-dependent MOF formation induced by different concentrations of D-Xylose (**4**) at different concentrations.

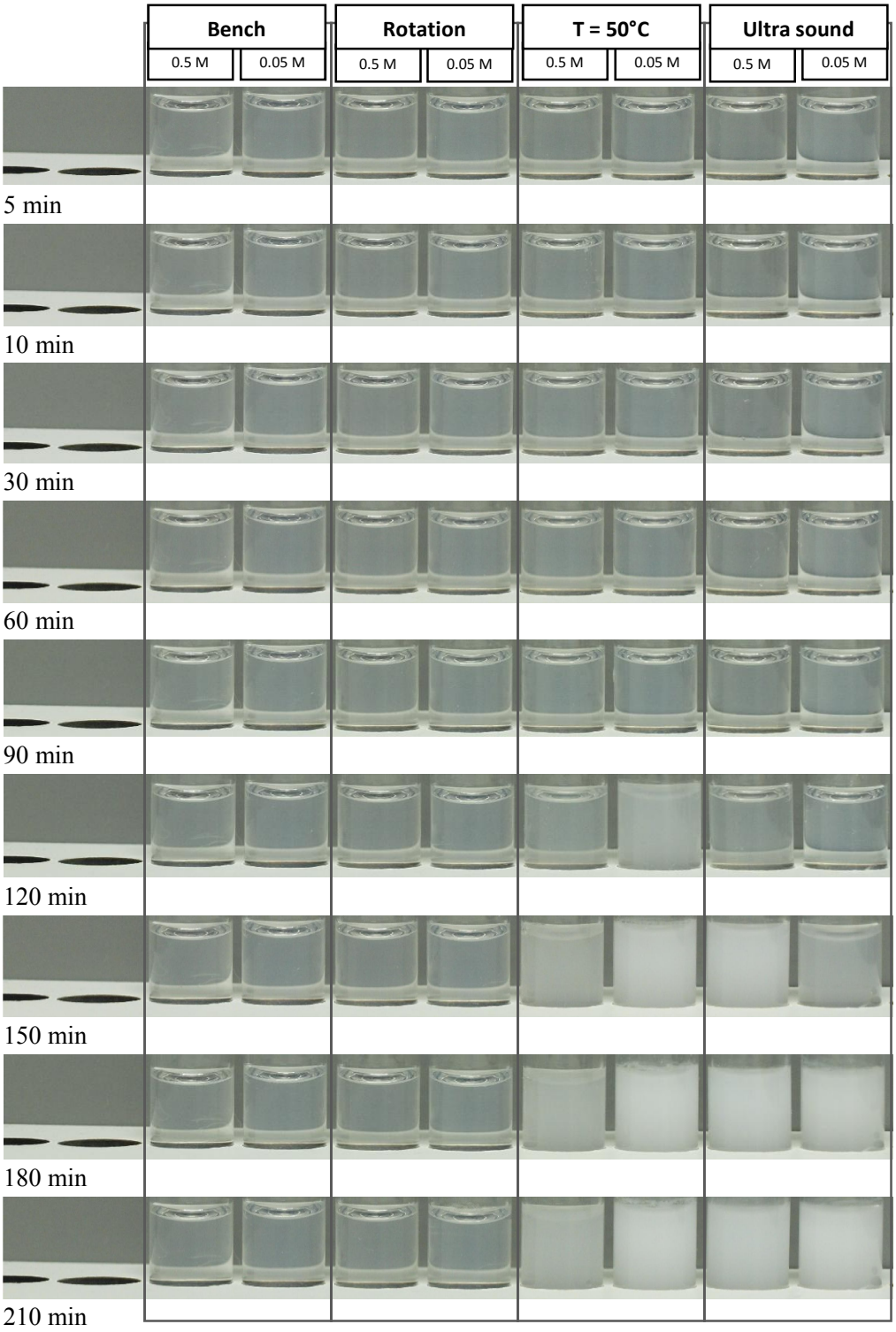

Figure S16. Comparison of different conditions during the MOF-synthesis supported by Methyl-α-D-glucopyranoside (**5**).

The influence of different conditions during the MOF-formation were also investigated. Reaction mixtures containing two different concentrations (0.5 M and 0.05 M in total) of Methyl-α-D-glucopyranoside (**5**), D-Glucitol (**6**) and Meglumine (**7**) were prepared. Samples were prepared using different conditions such as: increased reaction temperature (T = 50°C); sonication, at room temperature; static conditions at room temperature; placed under rotation at room temperature. For all these conditions, the time depending appearance is summarized in **Figure S17–S18.**

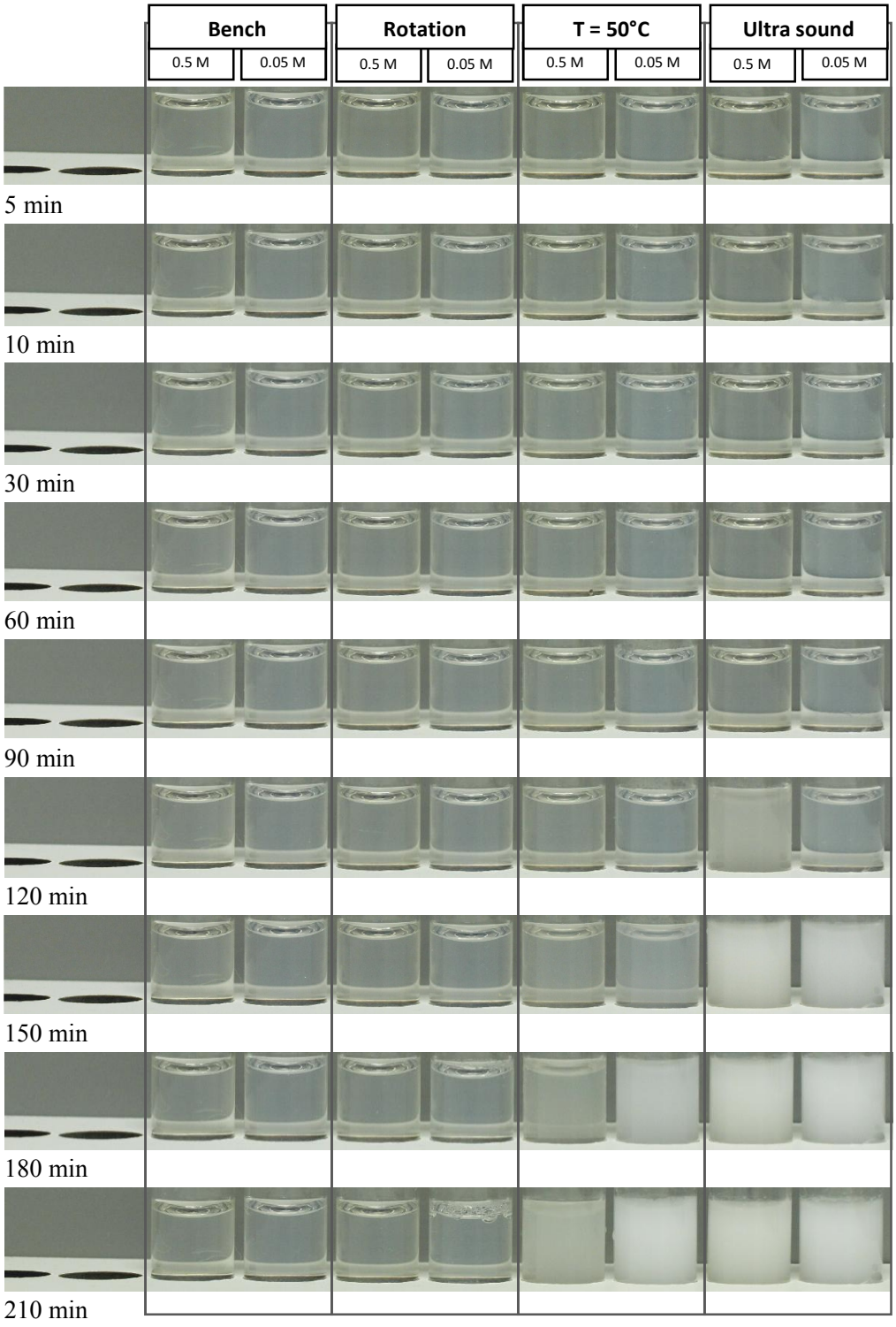

Figure S17. Comparison of different conditions during the MOF-synthesis supported by Glucitol (**6**).

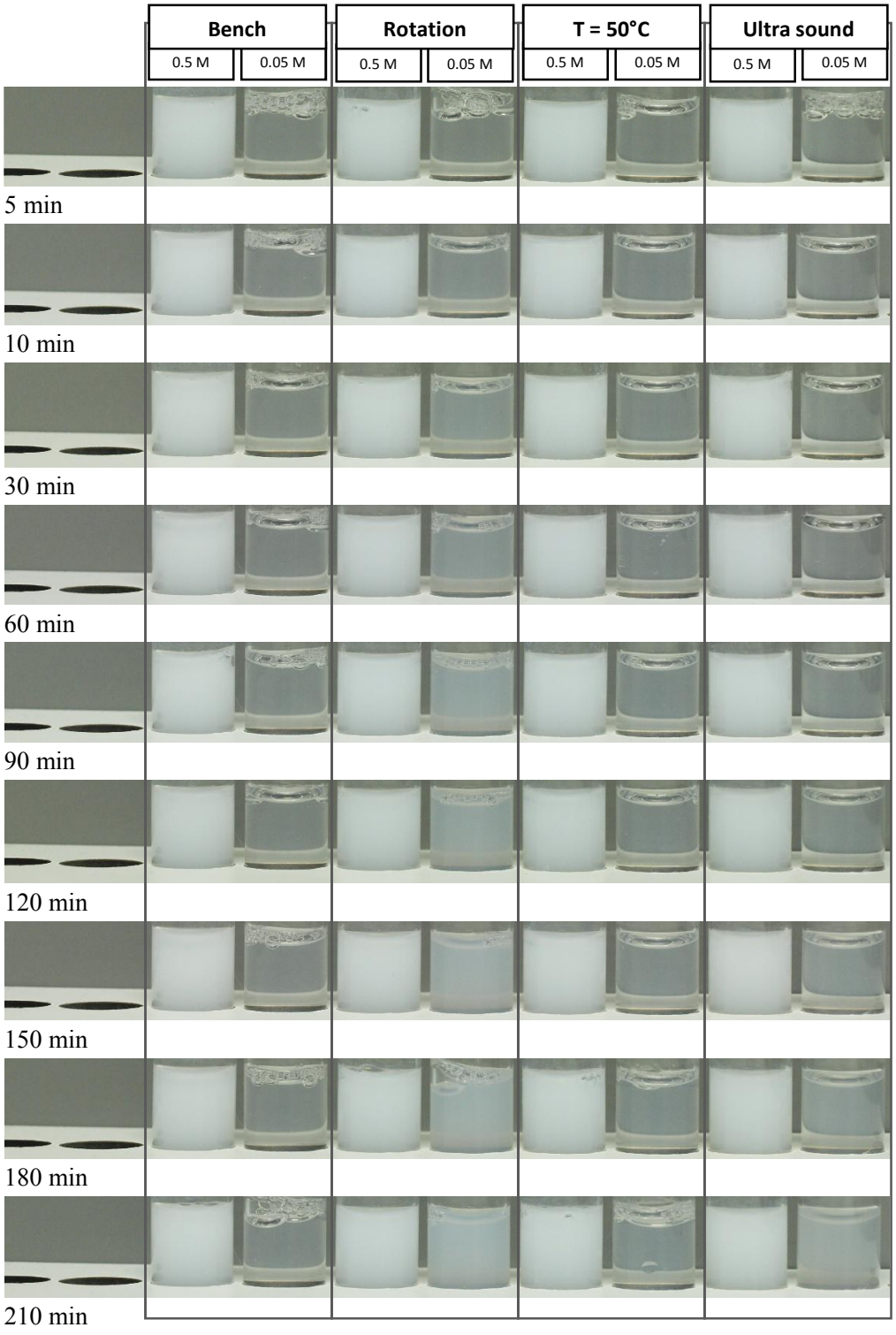

Figure S18.Comparison of different conditions during the MOF-synthesis supported by Meglumine (**7**).

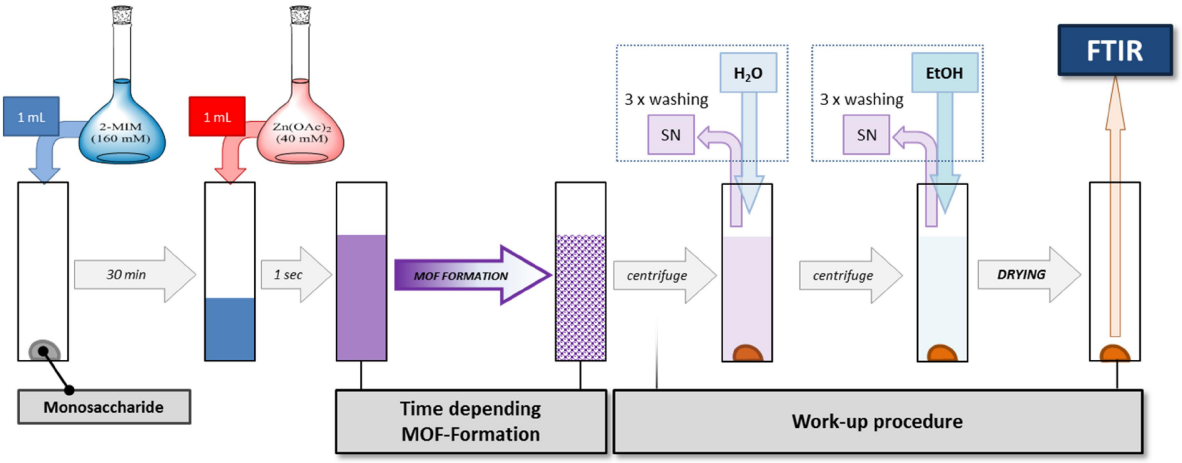

Figure S19. Schematic overview of the general procedure for the preparation of zeolitic frameworks.

For the investigations towards the encapsulation of monosaccharides, several reaction mixtures containing potential monosaccharides were prepared as described above (see **Figure S1**). After 15 hours (and under the premise, that a significant amount of precipitate was formed), the resulting reaction mixture was centrifuged (4500 rpm, 8 min). After the supernatant was removed, the remaining residue was washed with distilled water (ca. 5 min) and centrifuged again. This step was repeated three times and subsequently performed with ethanol instead of the water. Finally, the resulting product was dried at ambient conditions for 24 hours (see **Figure S19**). FTIR-spectroscopy of the obtained powders (**Figure S20-S22**) provide clear evidence that all the attempt in encapsulating saccharides failed as the vibrational modes are related to pure zeolitic Imidazolate framework materials.

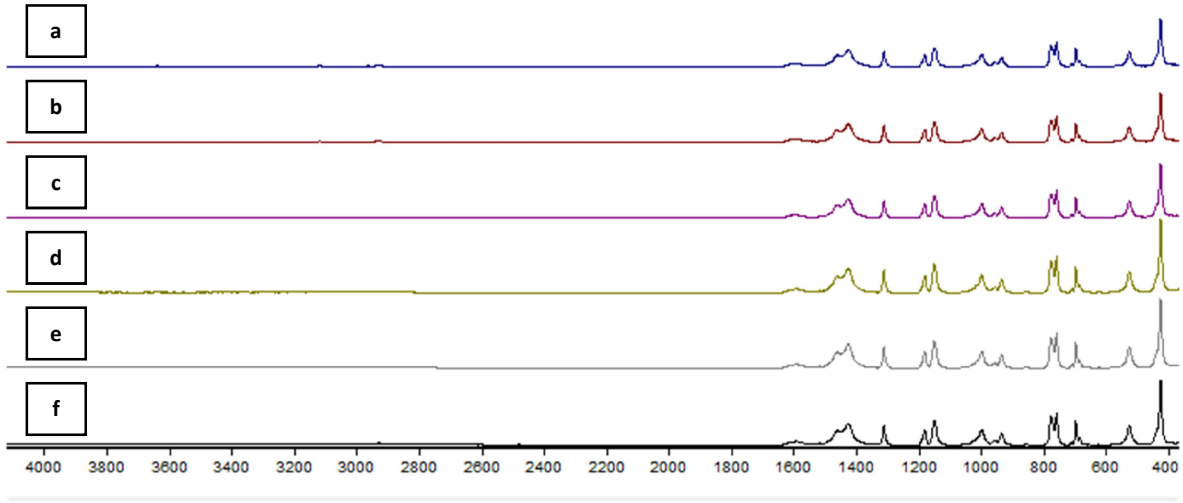

Figure S20. FTIR-spectra of the observed products.

a) D-Glucose (**1**, c = 1.25 M), **b**) D-Gluconic acid-δ-lactone (**11**, c = 0.005 M), **c**) Meglumine (**7**, c = 1.25 M), **d**) D-Glucosamine hydrochloride (**9**, c = 0.005 M), **e**) *N*-Acetyl-D-glucosamine (**8**, c = 0.625 M), **f**) D-Xylose (**4**, c = 1.25 M).

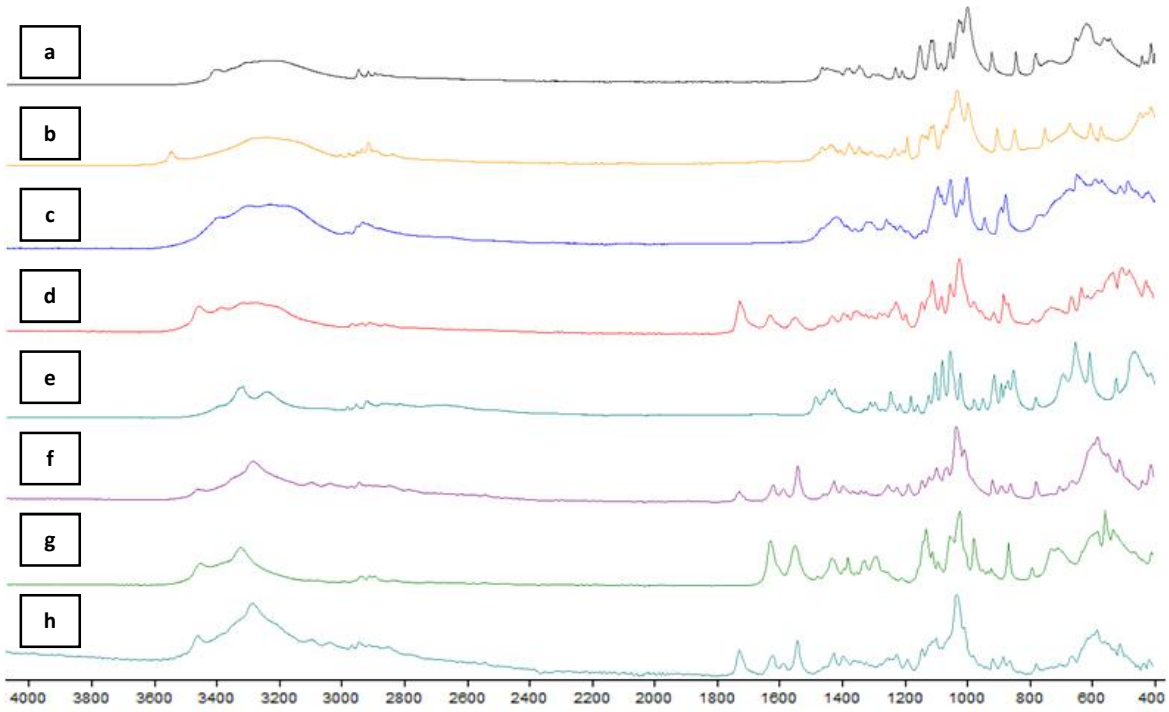

Figure S21. FTIR-spectra of the respective tested monosaccharides.

a) D-Glucose (**1**), **b**) Methyl-α-D-glucopyranoside (**5**), **c**) D-Glucitol (**6**), **d**) D-Gluconic acid-δ-lactone (**11**), **e**) Meglumine (**7**), **f**) D-Glucosamine hydrochloride (**9**), **g**) *N*-Acetyl-D-glucosamine (**8**), **h**) D-Xylose (**4**).

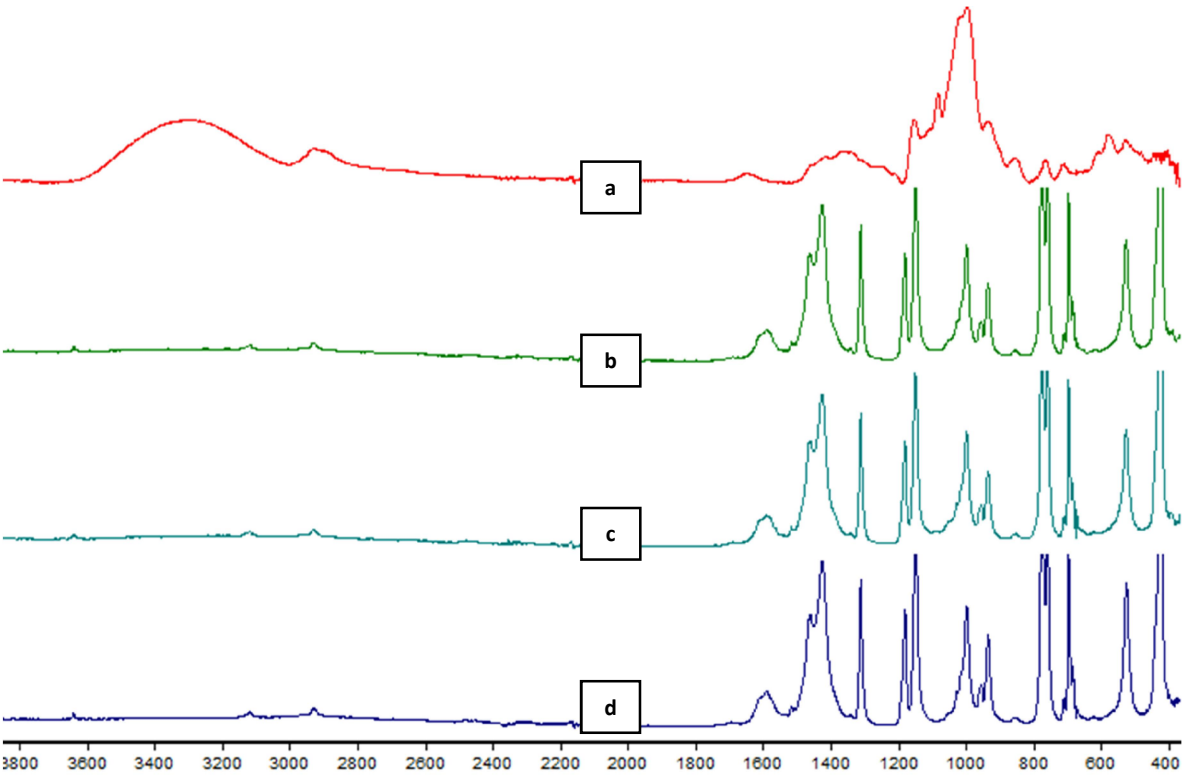

Figure S22. FTIR-spectra of: a) Maltodextrin, compared with the obtained products b) 5 mg/mL, c) 10 mg/mL, and d) 20 mg/mL of Maltodextrin supported ZIF-8 formation.

In a typical experiment Maltodextrin in the respective amount 5, 10 and 20 mg/mL) was dissolved in 7 mL 2mIM (initial concentration = 160 mM). Then aqueous solution of 7 mL $Zn(OAc)_2$ (initial concentration = 40 mM) was added at room temperature. The solutions were stirred overnight at room temperature. The precipitates were collected by centrifugation, washed wit DI water (3X) and ethanol (3X). The resulting powders were dried for FTIR characterisation. The reaction was performed 3 times to proof its reproducibility.

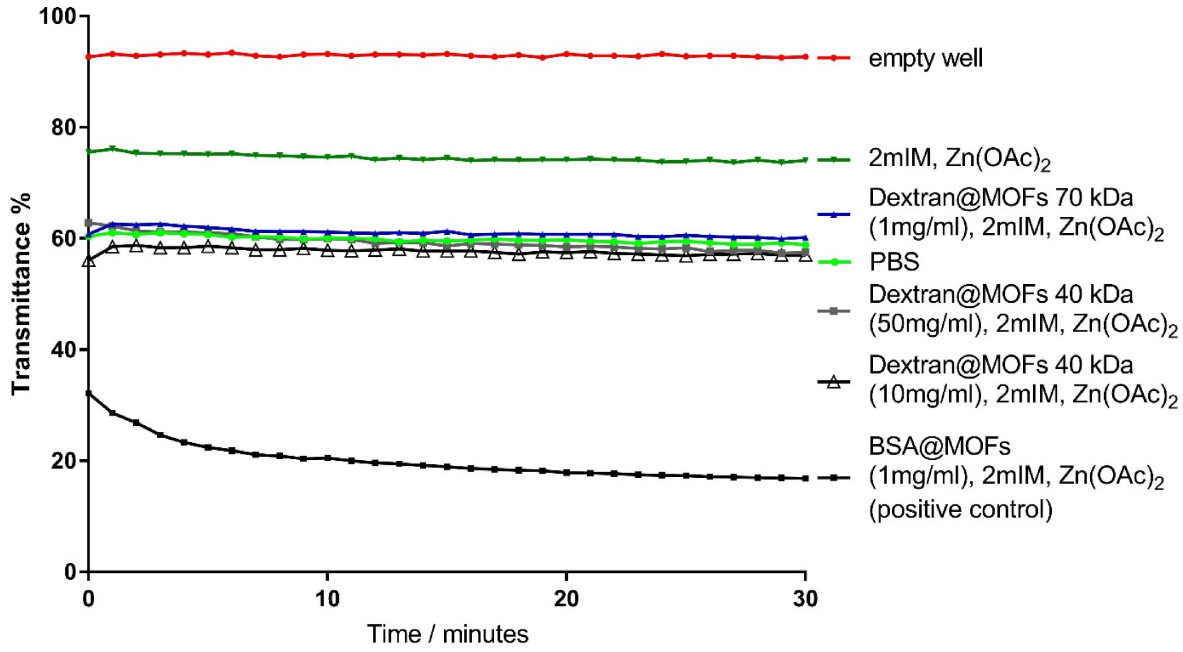

Figure S23. Kinetic tests using different Dextrans at various concentrations for the investigation of their biomimetic mineralization effects.

The test was performed adding Dextrans in an aqueous solution of 2mIM and $Zn(OAc)_2.2H_2O$ The kinetic was monitored using a plate reader (595 nm). Three negative controls were used: 1) the empty well, 2) the aqueous mixture of 2mIM and $Zn(OAc)_2$ mixed in water and 3) PBS buffer solution. As a positive control BSA was used to test the biomimetic mineralization adding the protein to an aqueous solution of 2mIM and $Zn(OAc)_2$. From this experiment, BSA demonstrated a significantly higher decrease in the transmittance due to the formation of BSA@MOFs.

Details of the experiment

30 µl of freshly-made 2mIM (13.1 mg/mL; 160 mM) and 30 µl of freshly-made $Zn(OAc)_2 \cdot 2H_2O$ (8.8 mg/mL; 40 mM) were pre-mixed with 30 µl of either Dextran 70 kDa (1 mg/mL), Dextran 40 kDa (10 mg/mL and 50 mg/mL) or BSA (1 mg/mL). Directly after mixing, the particle formation was investigated using a plate reader (FLUOstar OTPIMA, BMG LABTECH), absorbance measurement at 595 nm for 30 min with 1 minute time frames, no shaking and at 37°C. The mean absorbance out of two independent runs was calculated and the mean absorbance was converted into % transmittance via antilog (2-absorbance). The graph was plotted using GraphPad Prism 7.02 and analysed via ANOVA followed by Tukey's multiple comparisons test. BSA@MOFs showed a highly significant increase in % transmittance compared to the Dextrans ($p=0.0001$).

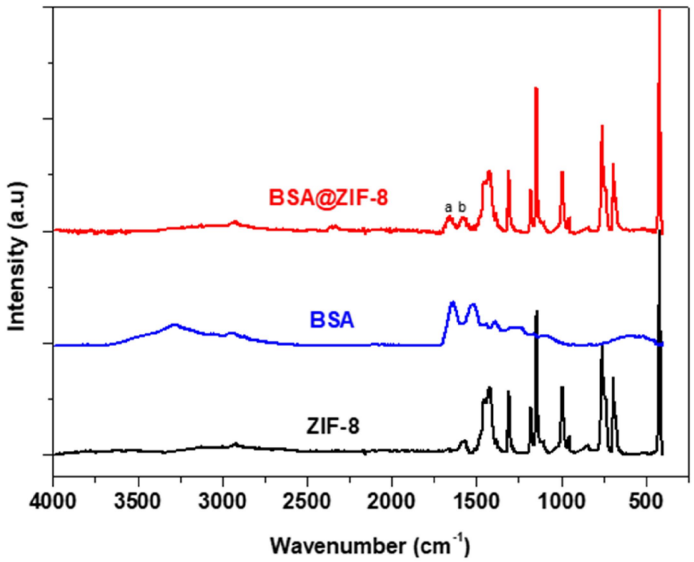

FTIR Spectra of BSA@MOF (1mg/mL BSA). Amide I (a) and Amide II (b).

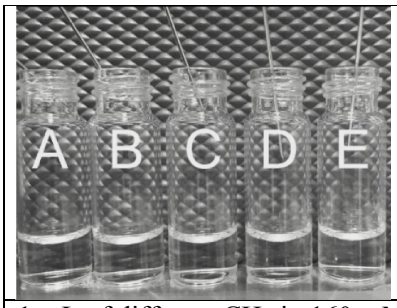	
1 mL of different CHs in 160 mM 2mIM.	Addition of 40 mM $Zn(OAc)_2$. Time=0
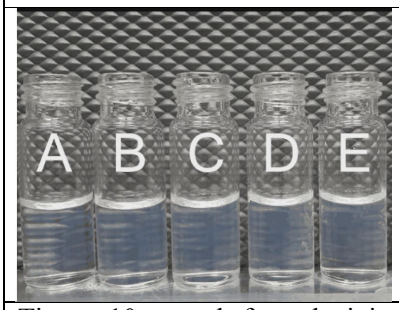	
Time = 10 seconds from the injection	Time = 30 seconds from the injection
	
Time = 2 minutes from the injection	Time = 4 minutes from the injection

Figure S24. Photographs of solutions using the polysaccharides with different molecular weights (Dextrans and Maltodextrin).

Photographs of solutions using the polysaccharides listed in table below. Composition and procedure: 1 mg of the respective carbohydrate (listed in **Table below**) was dissolved in 1 mL of a freshly prepared 2mIM solution (160 mM in DI water) at ambient temperature (Figure S24). After 30 min, the 1 mL of the 2nd precursor solution ($Zn(OAc)_2$, 40mM in DI water) was added at once in all vials (Figure S24).

Table of CHs with different molecular weights (Dextrans and Maltodextrin)

Sample		**MW (g/mol)**	**comment**
A	Blank	-	NO polysaccharide added
B	Maltodextrin	3.000-4.000	-
C	Dextran	6.000	-
D	Dextran	40.000	-
E	Dextran	70.000	-

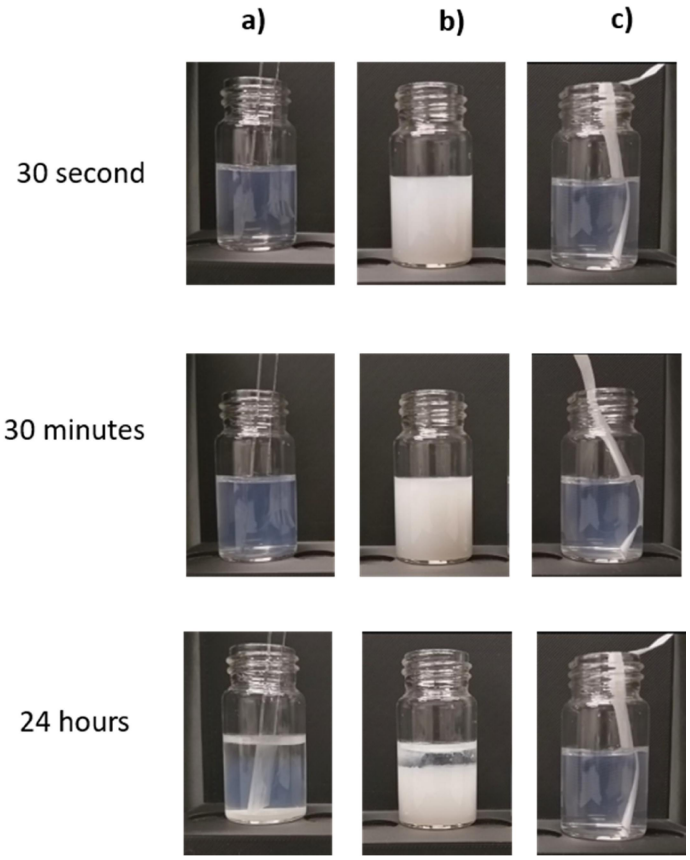

Figure S25. Screenshot of synthesis of ZIF-8 with the Zn^{2+}:2mIM = 1:4 at 30 second, 30 minutes and 24 hours on paper and glass plate.

The solution of 2mIM (160 mM) was mixed by $Zn(OAc)_2$ (40 mM) and a glass plate **a)**, the next vial contains of 2mIM (160 mM) and CM-dextran (0.36 mg /mL) was mixed by $Zn(OAc)_2$ (40 mM) **b)**, the last vial contains 2mIM solution (160 mM) was mixed by $Zn(OAc)_2$ (40 mM) and a piece of paper (S&S filter paper 110 mm) **c)**.

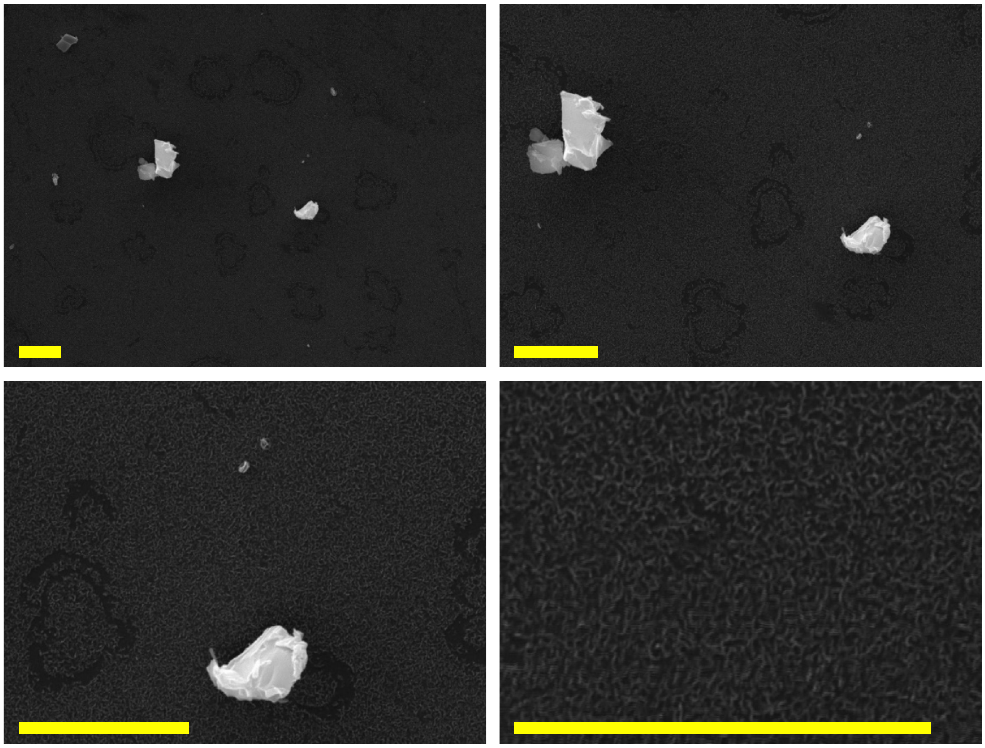

Figure S26. SEM image of the product using Zn^{2+}:2mIM = 1:4 on glass surface after 30 second (scale bar = 25 μm).

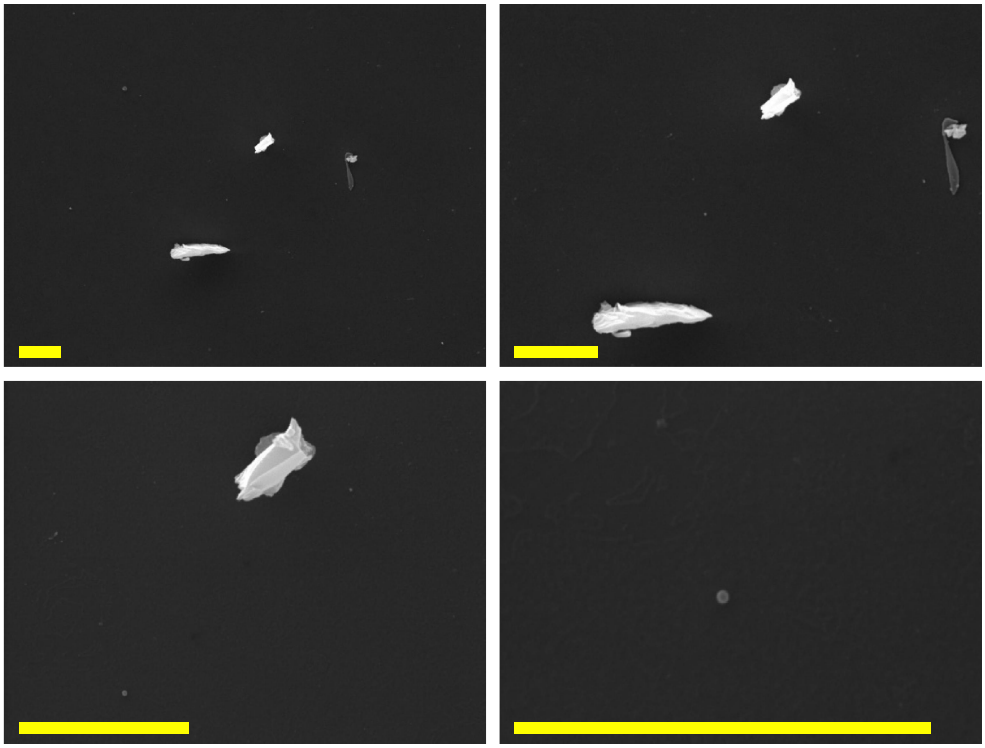

Figure S27. SEM image of the product using Zn^{2+}:2mIM = 1:4 on glass surface after 30 minutes (scale bar = 25 μm).

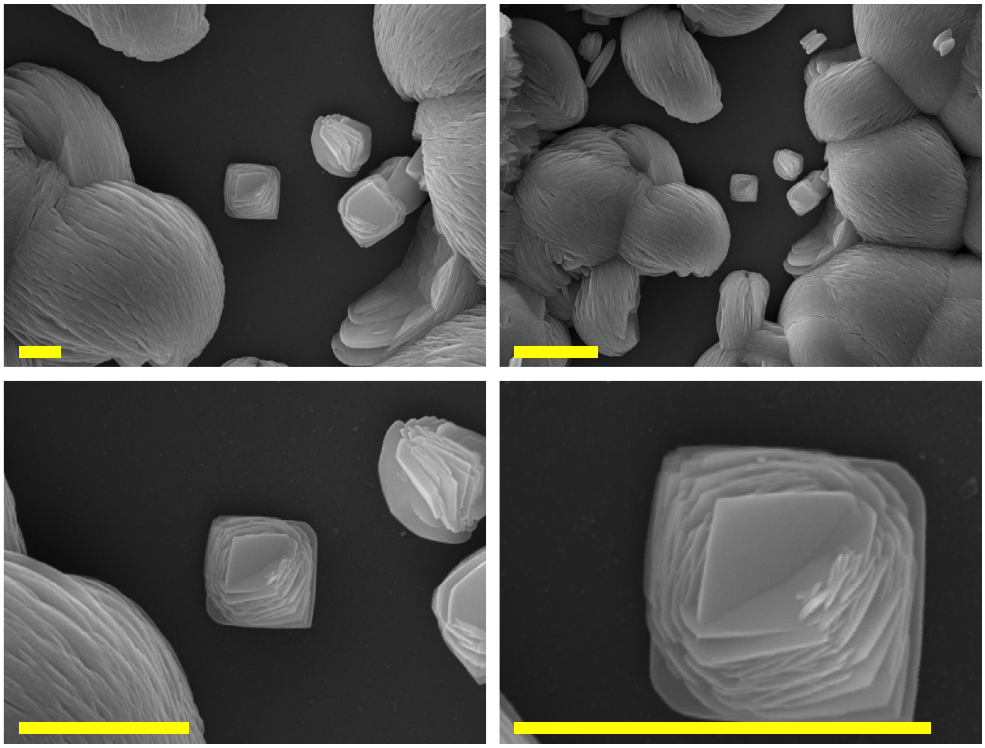

Figure S28. SEM image of the product using Zn^{2+}:2mIM = 1:4 on glass surface after 24 hours (scale bar = 25 μm).

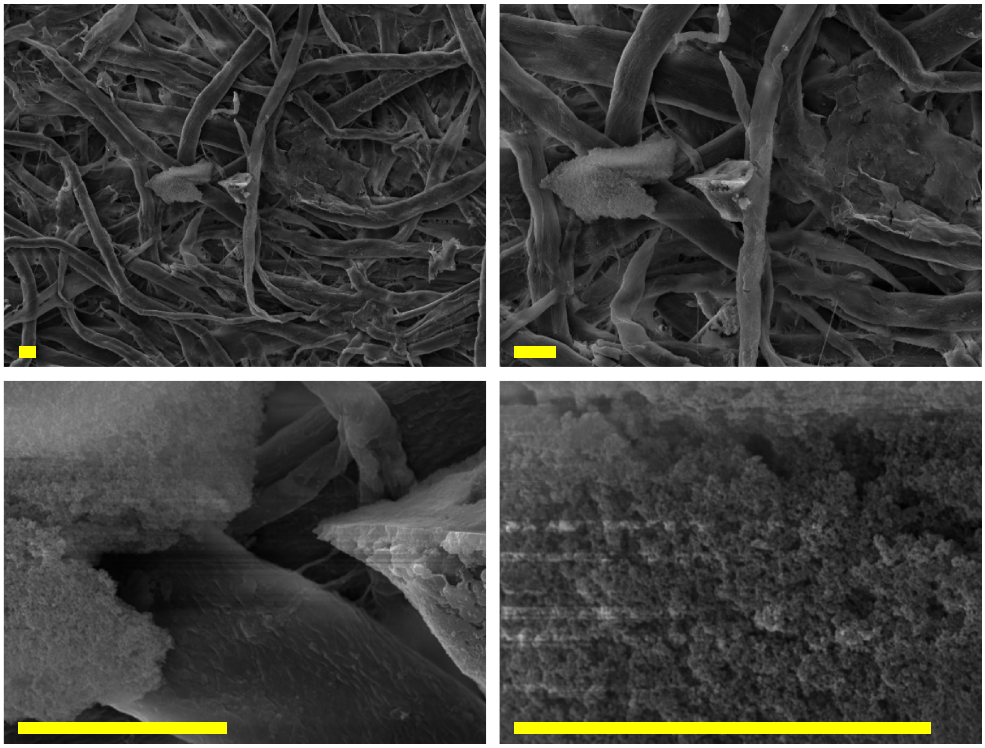

Figure S29. SEM image of the product using Zn^{2+}:2mIM = 1:4 on paper after 30 second (scale bar = 25 μm).

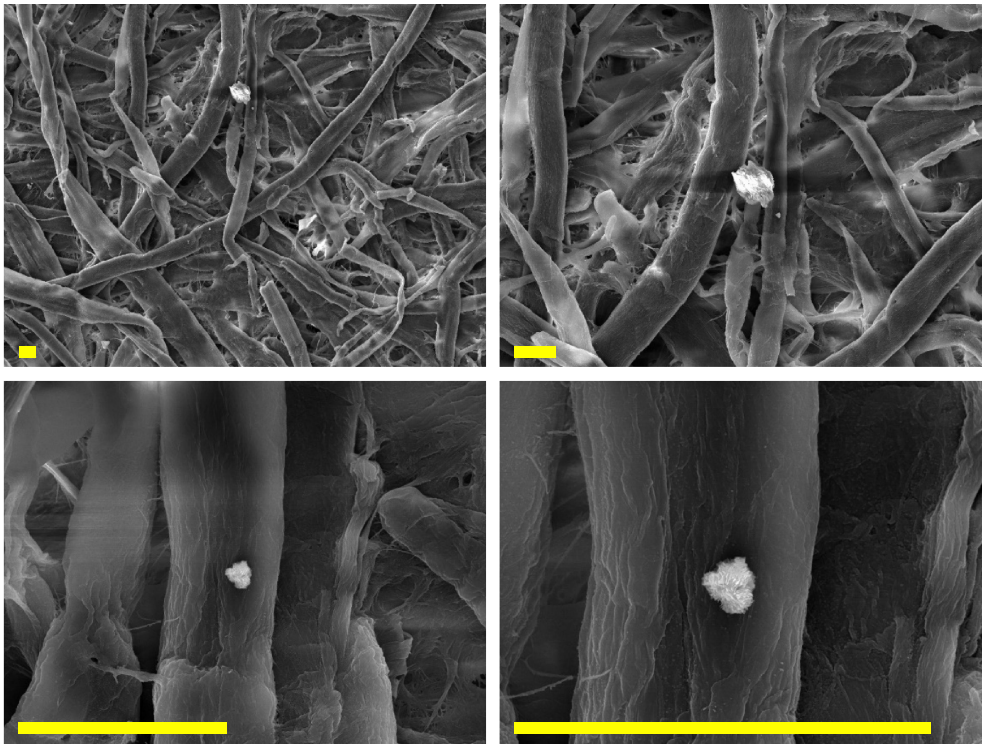

Figure S30. SEM image of the product using Zn^{2+}:2mIM = 1:4 on paper after 30 minutes (scale bar = 25 μm).

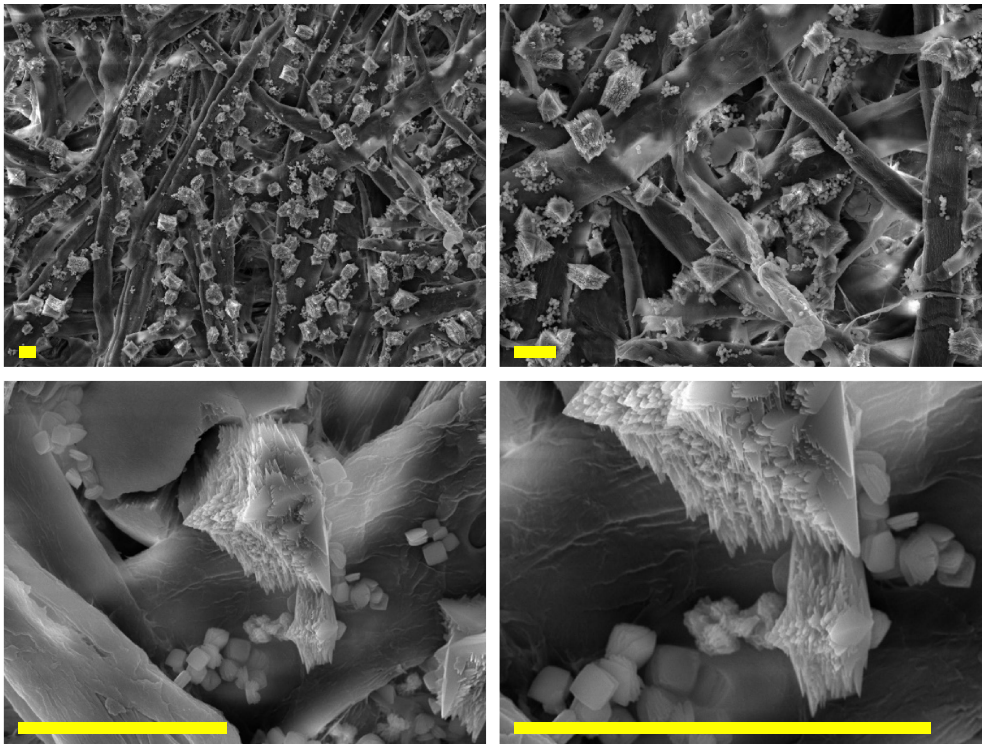

Figure S31. SEM image of the product using Zn^{2+}:2mIM = 1:4 on paper after 24 hours (scale bar = 25 μm).

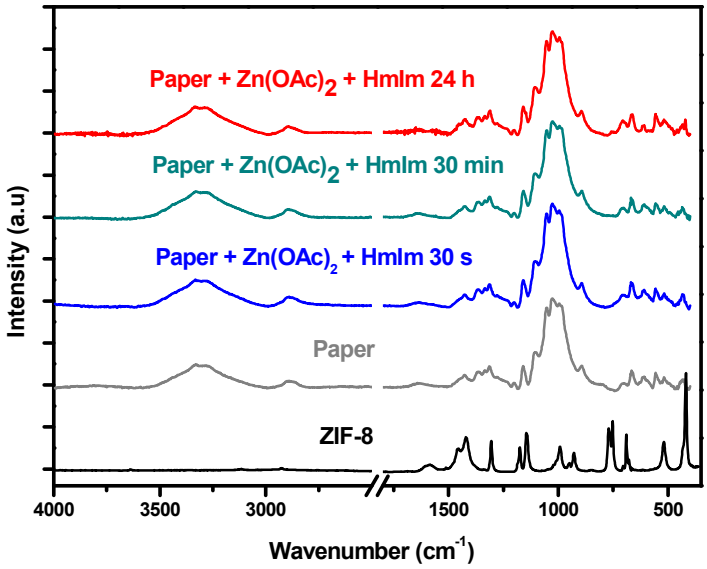

Figure S32. FTIR Spectra of paper (S&S filter paper 110 mm) with Zn^{2+}:2mIM = 1:4 after 30 second, 30 minutes and 24 hours compared with ZIF-8.

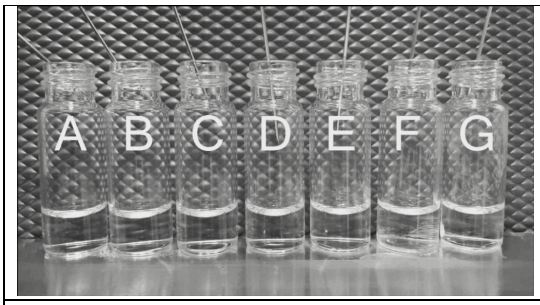	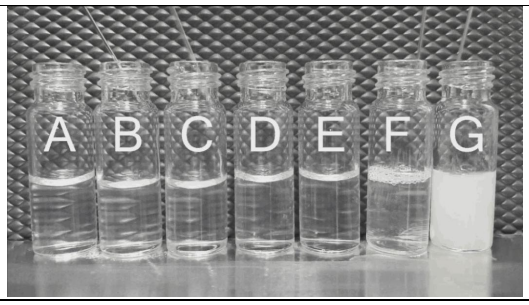
1 mL of different CHs in 160 mM 2mIM.	Addition of 40 mM $Zn(OAc)_2$. Time=0
	
time = 10 seconds from the injection	Time = 30 seconds from the injection
	
Time = 2 minutes from the injection	Time = 4 minutes from the injection

Figure S33. Photographs of solutions using the polysaccharides with different molecular weights and chemical functionalizations.

The video is available as supporting information. Photographs of solutions using the polysaccharides listed in table on the next page. Composition and procedure: 1 mg of the respective carbohydrate (listed in Table on the next page) was dissolved in 1 mL of a freshly prepared 2mIM solution (160 mM in DI Water) at ambient temperature (Figure S33). After 30 min, 1 mL of the 2nd precursor solution ($Zn(OAc)_2$, 40mM in DI water) was added at once in all vials (Figure S33).

Table of CHs with different molecular weights and chemical functionalizations

Sample		**MW (g/mol)**	**comment**
A	Blank	-	NO polysaccharide added
B	Maltodextrin	3.000-4.000	-
C	Dextran	6.000	-
D	Dextran	40.000	-
E	Dextran	70.000	-
F	Diethylaminoethyl dextran	10.000	2.5-4.5% nitrogen; (ca. one substituent on every 3rd glucose unit)
G	Carboxymethyl dextran sodium salt	10.000-20.000	1.1-1.5 mmol/g; (ca. one substituent on every 3rd glucose unit)

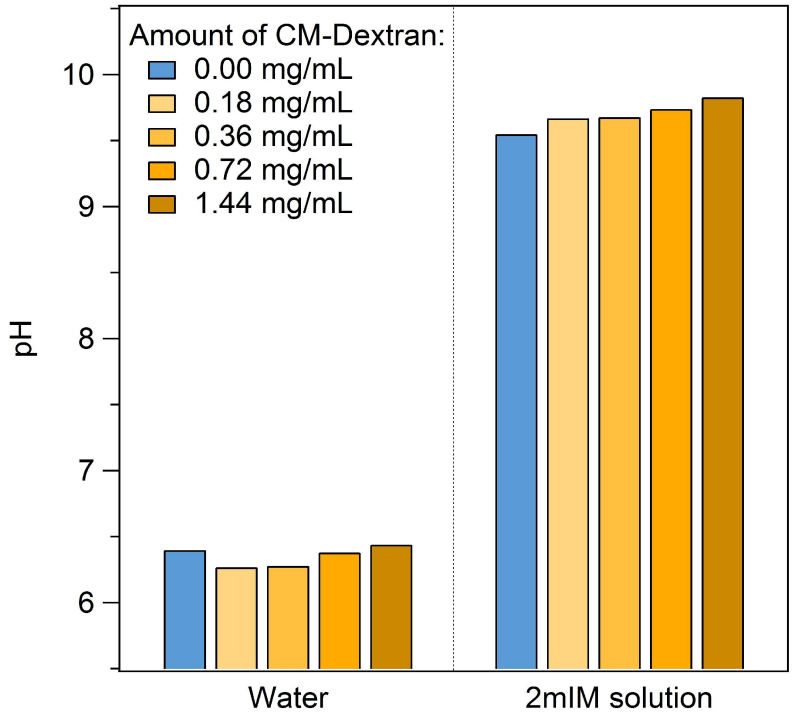

Figure S34. The pH of CM-dextran (0, 0.18, 0.36, 0.72, 1.44 mg/mL) in H_2O and 2mIM solutions with total volume 2 mL.

The pH for solutions prepared according to the volumes and the concentrations used for the synthesis of CM-dextran@ZIF-8. Based on the values of the pH measured with respect to the control samples (no CM-dextran), it does not seem that the CM-dextran plays a significant role in the deprotonation of the ligand. However, the ligand itself changes the pH from 6.4 (water) to c.a. 9.5 (mixture 2mIM in water).

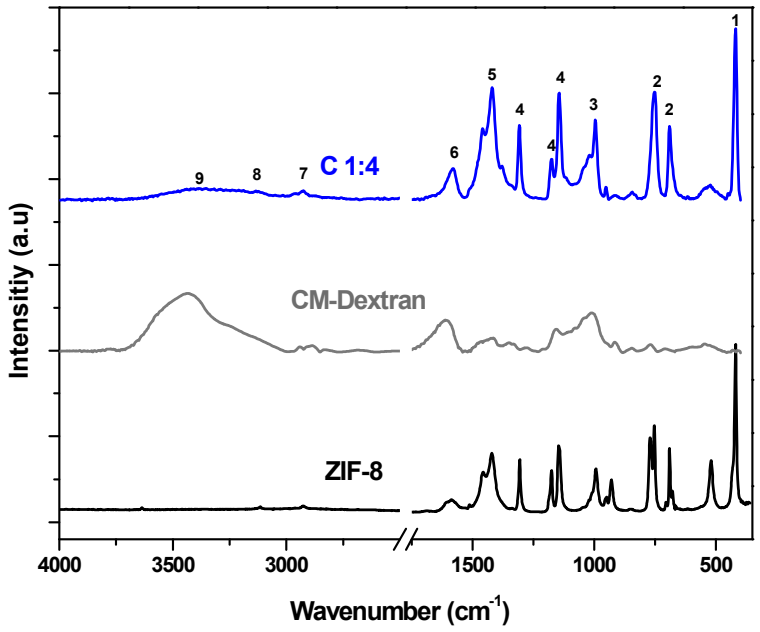

Figure S35. FTIR spectra of CM-dextran@ZIF-8 (Zn^{2+}:2mIM = 1:4)

The assignment of the vibrational modes is reported in the table below.

Table of FTIR interpretation of CM-dextran@ZIF-8

No	Characteristic Absorptions (cm^{-1})	Functional Group	References
1	421	Zn-N stretching	[2]
2	600-800	Out plane bending of the 2mIM ring	[2 3]
3	900-1350	In plane bending of the 2mIM ring	[2 3]
4	997	C-O stretching of CM-dextran	[4]
5	1420	Entire ring stretching of 2mIM	[5]
6	1608	COO^- of CM-dextran	[6 7]
7	2926	Aliphatic C-H stretching of 2mIM	[5]
8	3120	Aromatic C-H stretching of 2mIM	[5]
9	2850-3600	O-H stretching	[8]

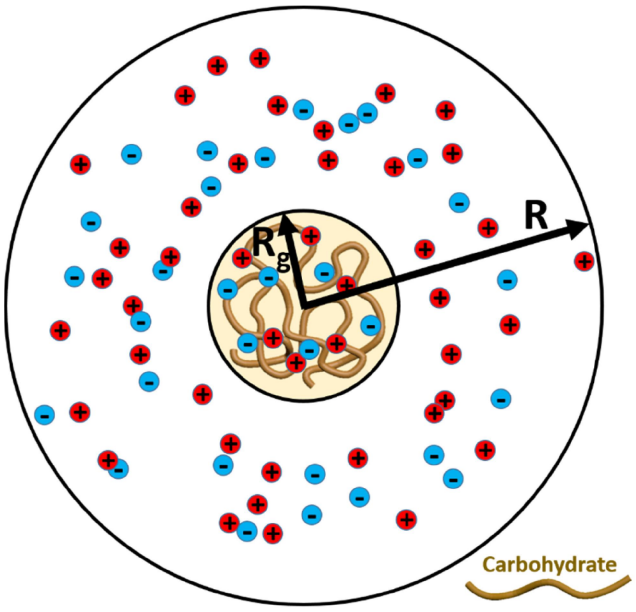

Figure S36. Schematic of the ion-permeable spherical model of a carbohydrate chain with a radius of gyration (R_g) in an electrolyte solution. The electrostatic potential was taken to be zero at a large distance, R, from the centre of the ion-permeable sphere.

We modelled a dextran chain as an ion-permeable sphere with a radius given by the radius of gyration (R_g) of a freely-jointed chain of length N segments (**Figure S36**),[9] since single molecule AFM studies of functionalized and native dextran chains have shown from their elasticity that they can be described approximately as freely-jointed chains with Kuhn lengths equal to the length of the glucose monomer (4.4 Å).[10,11] Therefore, the number of segments, N, was equal to the degree of polymerization (DP)[9]. Although branching is common for dextran chains, the branching density of the experimental sample was unknown, so for simplicity we assumed that the dextran chain in our model was unbranched. Nevertheless, we do not expect the conclusions from the model to change significantly if branching was considered. We applied the ion-permeable sphere model because most of the pervaded volume will be accessible to ions in solution (the average separation of monomers in the pervaded volume ≈ 5.7Å, whereas the diameter of Zn^{2+} ion is 1.48 Å and the diameter of the acetate counter-ion is ≈ 3.72 Å)[12,13]. Table S6 below shows the parameters used.

Table S6. Parameters of the ion-permeable sphere model of dextrans.

parameter	value
carbohydrate concentration	0.72 mg mL^{-1}
degree of polymerisation (DP)	60
Kuhn length (l_k)	4.4 Å[10]
polymer molecular weight (M)	≈ 10kDa
radius of gyration (R_g)	13.91 Å
bulk zinc concentration ($c_{+,\,bulk}$)	0.04 M
pK_a of CM	4.0
pK_a of AM	10.64[14]
pH	11

Under the standard ZIF-8 synthesis conditions used throughout this work, the bulk zinc ion (Zn^{2+}) concentration ($c_{+,\,bulk}$) is 0.04 M and the concentration of counter ions, with a valency of -1, is 0.08 M. The Debye length (λ_D) is

$$\lambda_D = \kappa^{-1} = \left(\frac{\varepsilon_r \varepsilon_0 k_B T}{2e^2 I}\right)^{1/2}, \quad \textbf{(S1)}$$

where ε_0 is the vacuum permittivity, ε_r is the relative permittivity of water (80), T is temperature (298 K), k_B is the Boltzmann constant, e is the elementary charge, and I is the ionic strength of the electrolyte solution, giving $\lambda_D = 8.86$ Å.

The average number of functionalized sites per glucose monomer is given by the degree of substitution (DS), α, which can take any value from 0 to 3. DS was approximately 0.125 in the experiments presented in this paper, which corresponds to 1 functionalized group every eight monomers. We calculated the total charge ($Q_\pm$) on a dextran chain as $Q_\pm = \alpha N q_\pm$, where $q_\pm$ is the average charge of a functional group on the chain, given by the Henderson-Hasselbach equation,

$$q_\pm = \pm \frac{10^{\mp \mathrm{pH} \pm \mathrm{p}K_a}}{10^{\mp \mathrm{pH} \pm \mathrm{p}K_a + 1}}, \quad \textbf{(S2)}$$

where the sign of $q_\pm$ is determined by the sign of the charge on the functionality (-1 for CM and +1 for AM). A range of values have been reported for pK_a of the CM functionality, but in all cases it is much smaller than the pH (≈ 11) used in the experiments. Thus, each CM functionality is expected to have a full negative charge under the experimental conditions. Furthermore, there are multiple amine species associated with the AM functionality and it is expected that each amine will have a different pK_a. For

simplicity, we have assumed a single pK_a value, representative of a tertiary amine,[14] which will be partially positively charged at the pH used in the experiments. The following figure shows the volume charge density ($\rho_s = \frac{3Q_\pm}{4\pi {R_g}^3}$) as a function of DS for both functionalities with the specified parameters (**Table S6**).

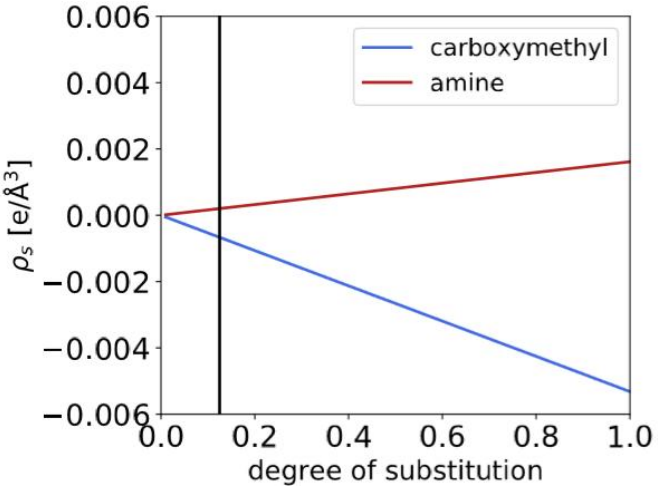

Figure S37. Volume charge density (ρ_s) of the ion-permeable spheres as a function of degree of substitution for carboxymethyl (CM) and amine (AM) functionalities. The black line represents the approximate DS used in the experiments.

We used the boundary value problem solver in the SciPy Python library[15] to solve the nonlinear Poisson-Boltzmann (PB) equation around an ion-permeable sphere,[16]

$$\nabla^2\psi = -\frac{e}{\varepsilon_r\varepsilon_0}\left[\sum_{i=\pm} c_{i,\,\mathrm{bulk}} z_i \exp\left(\frac{-z_i e\psi}{k_\mathrm{B}T}\right)\right] - \frac{\rho(r)}{\varepsilon_r\varepsilon_0}, \qquad \textbf{(S3)}$$

where ψ is the electrostatic potential at the radial coordinate r, $c_{\pm,\,\mathrm{bulk}}$ and $z_\pm$ are the bulk concentration and valency of the positive zinc ions ($c_{+,\,\mathrm{bulk}} = 0.04$M and $z_+ = +2$) and negative acetate ions ($c_{-,\,\mathrm{bulk}} = 0.08$M and $z_- = -1$) in solution, respectively, and $\rho(r)$ is the charge density due to the carbohydrate chain, given by

$$\rho(r) = \begin{cases} \rho_s, & \text{if } 0 \le r \le R_g \\ 0, & \text{if } r > R_g \end{cases}. \qquad \textbf{(S4)}$$

The following boundary conditions were applied to Equation S3:

$$1.\ \lim_{r\to 0}\frac{d\psi}{dr} = 0 \qquad \textbf{(S5)}$$

$$2.\ \psi(r = R) \to 0 \qquad \textbf{(S6)}$$

R was set to a large enough value (100 Å) such that its specific value did not affect the calculated potential or ion concentration near the ion-permeable sphere. We also applied the analytical solution to the linearized PB equation for an ion-permeable sphere reported by Ohshima and co-workers.[17] We note that the linearized

PB equation is only applicable when $|\psi| \ll \frac{k_B T}{z_+ e} \approx 12$ mV. Therefore, numerical solutions to the nonlinear PB equation were required in general. At low DS values ($\alpha < 0.04$), where the assumptions of the linearized PB equation are expected to hold, we found good agreement between the analytical and numerical results. For numerical stability, we replaced the step-function form of $\rho(r)$ in Equation 4 by the smooth function

$$\rho(r) = -\frac{\rho_s}{2}\left[\tanh\left(\frac{r - R_g}{2w}\right) - 1\right], \quad \textbf{(S7)}$$

where w defines the width of the transition of $\rho(r)$ from ρ_s to 0. w was set to $0.02\lambda_D$ and the final enhancement results were found to be robust to changes in w in the range $0.01\lambda_D \leq w \leq 0.5\lambda_D$.

From the electrostatic potential calculated using the PB equation, the concentration of zinc ions, $c_+(r)$, at radial coordinate r was calculated using

$$c_+(r) = c_{+,\,\text{bulk}} \exp\left[\frac{-z_+ e\psi(r)}{k_B T}\right]. \quad \textbf{(S8)}$$

The zinc ion enhancement at radial coordinate r is the ratio $\frac{c_+(r)}{c_{+,\,\text{bulk}}}$.

The electrostatic potential and zinc ion enhancement is reported at $r = 0$ (in Figures 2c and S37) because the approximate size of the MOF precursors (Zn^{2+} diameter = 1.48 Å and 2mIM diameter ≈ 5.2 Å) are smaller than the average separation of monomers in the pervaded volume (≈ 5.7Å). Therefore, it is possible that ZIF formation would occur anywhere within the pervaded volume of the carbohydrate chain. Thus, it can reasonably be expected that ZIF formation will be governed by the electrostatic potential and zinc ion enhancement at the centre of the ion-permeable sphere where the zinc ion concentration is greatest, but we note that ZIF growth could be seeded at any point for $0 \leq r \leq R_g$.

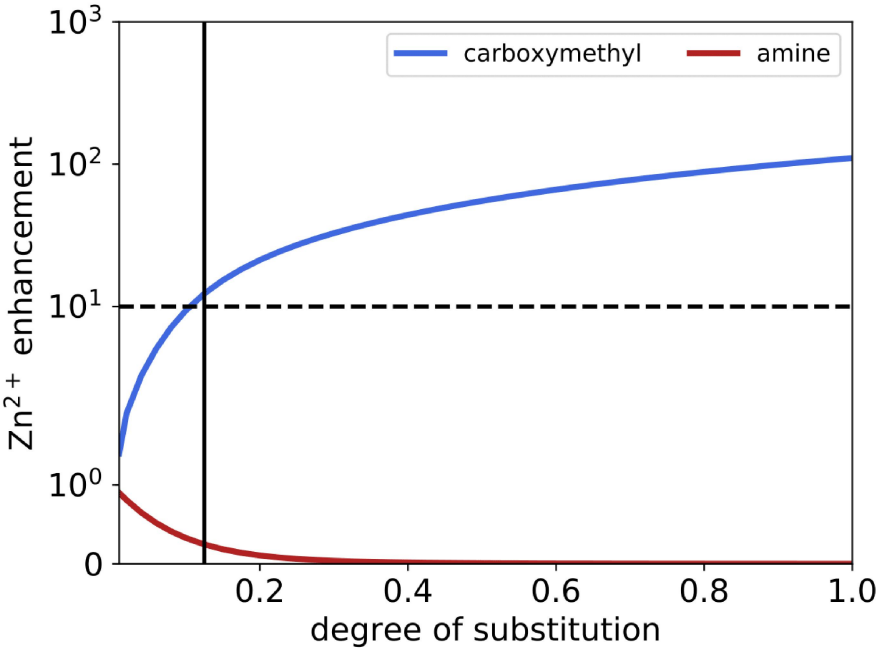

Figure S38. Calculated Zn^{2+} ion enhancement at the center of the carbohydrate versus degree of carboxymethyl or amino functionalization.

The code used for all calculations is available at https://bitbucket.org/andrewtarzia/sugar_source/

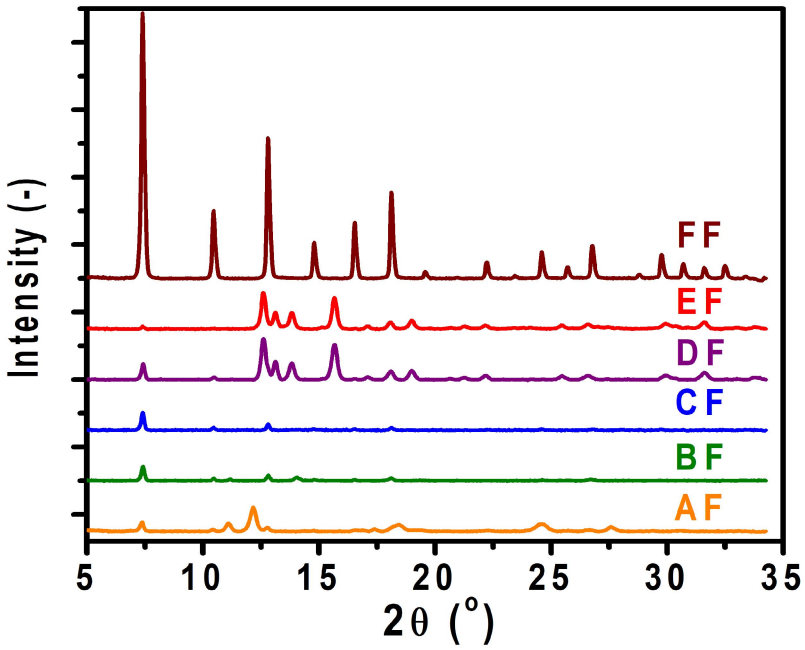

Figure S39. XRD of the FITC-CM-dextran@ZIF-8 biocomposites obtained with different metal-to-ligand ratios (AF = 1:2.52, BF = 1:3.47, CF = 1:4, DF = 1:6, EF = 1:8, FF=1:16).

The samples were synthesized analogous to synthesize CM-Dextran@ZIF-8, but using the FITC-CM-dextran in place of CM-dextran. The precipitates were collected by centrifugation and washed with H_2O and EtOH and dried in ambient temperature. AF found to be a mixture of phases, dominated by U12, BF and CF are predominantly sod, DF, and EF were a mixture of dia- and sod-Zn(mIM)$_2$ phases, while FF was found to be pure sod-Zn(mIM)$_2$.

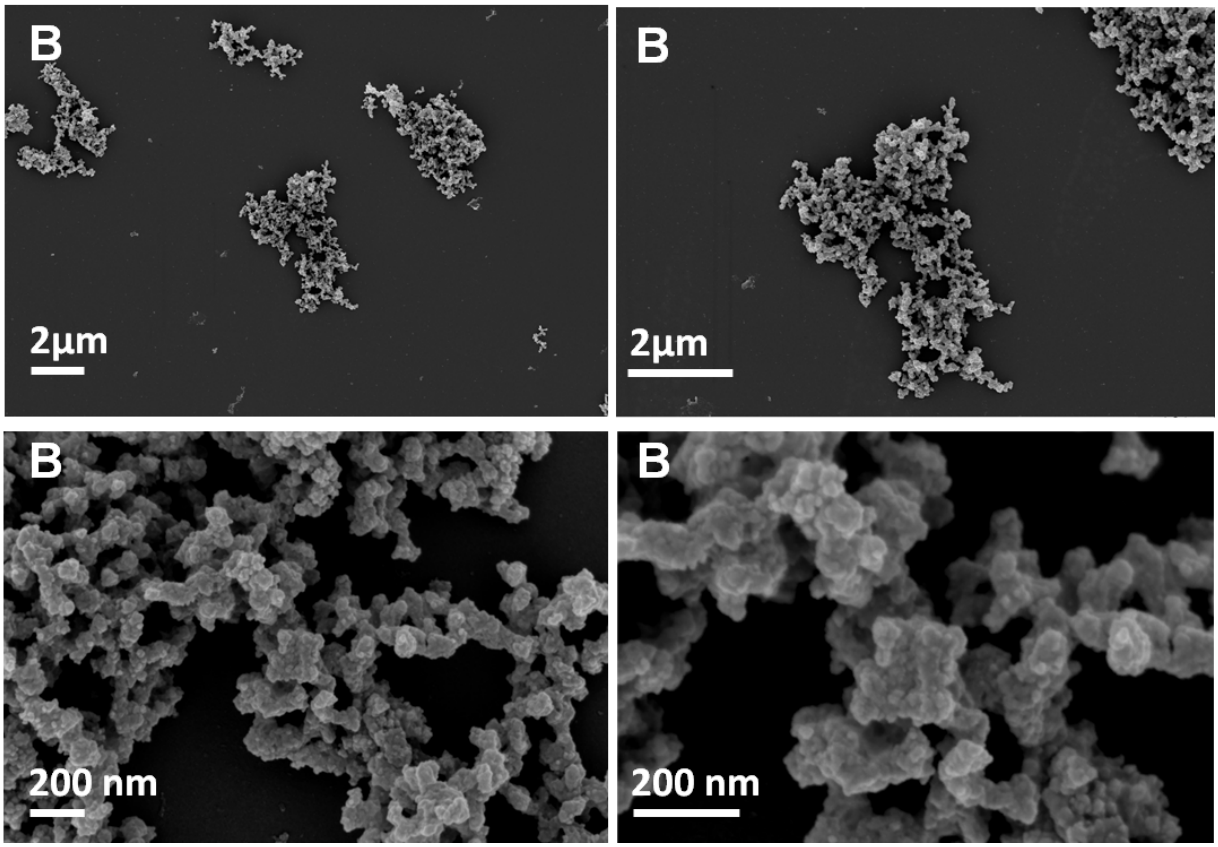

Figure S40. SEM images of B sample (Zn^{2+}:2mIM = 1:3.47).

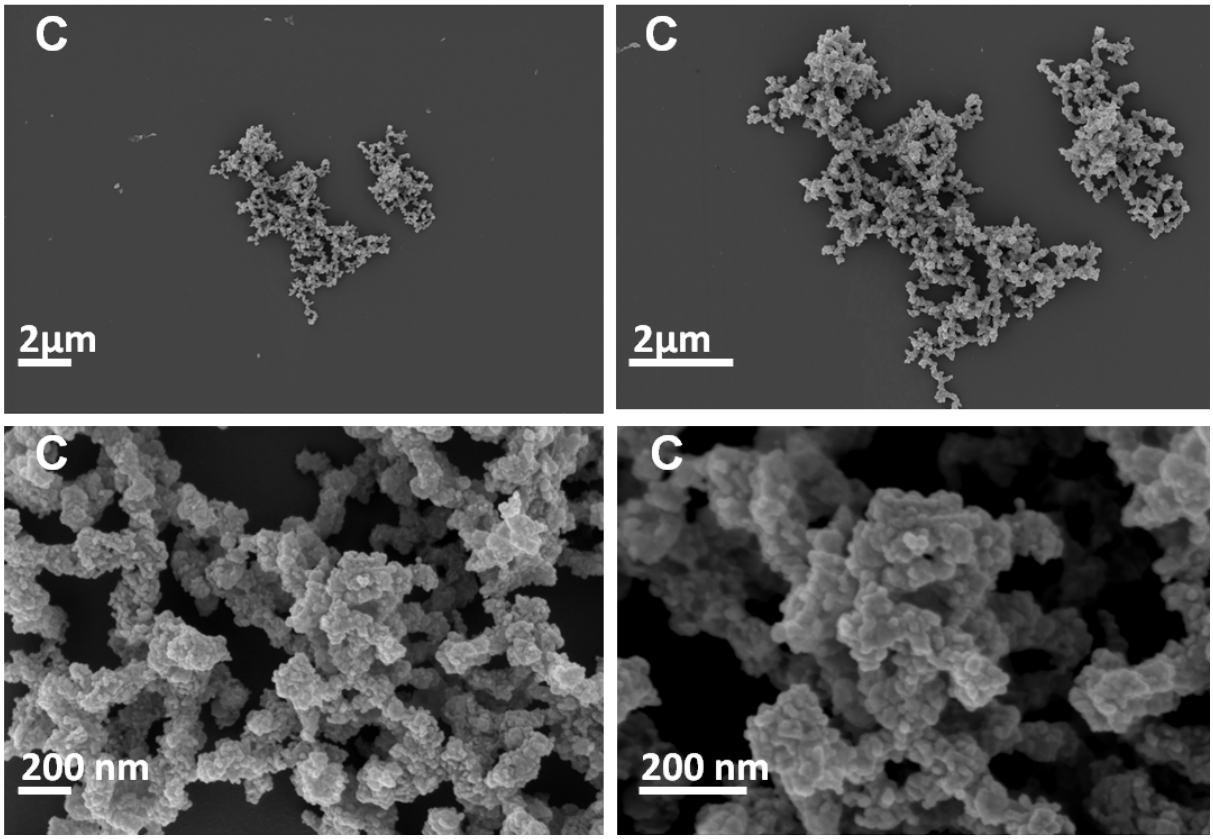

Figure S41. SEM images of C sample (Zn^{2+}:2mIM = 1:4).

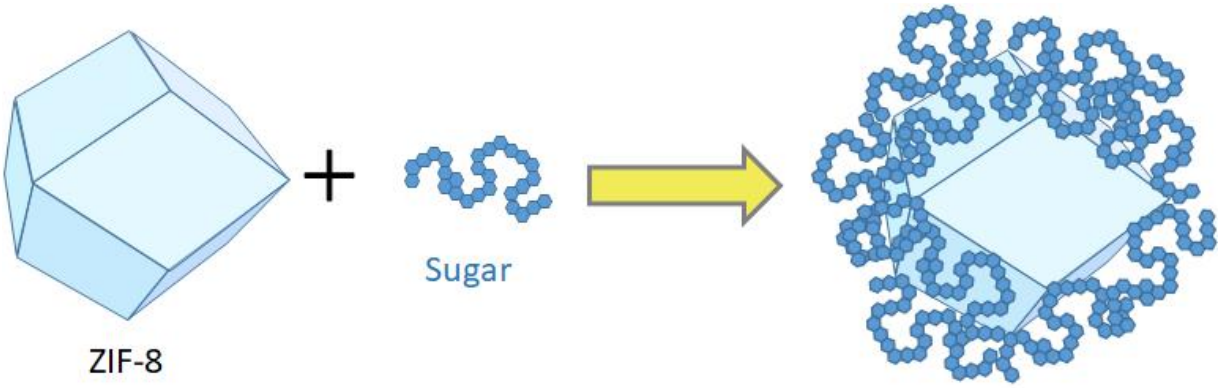

Figure S42. Schematic illustration of sugar on the surface of ZIF-8.

This was used for the optimization of the washing procedure (for the detail see page 5).

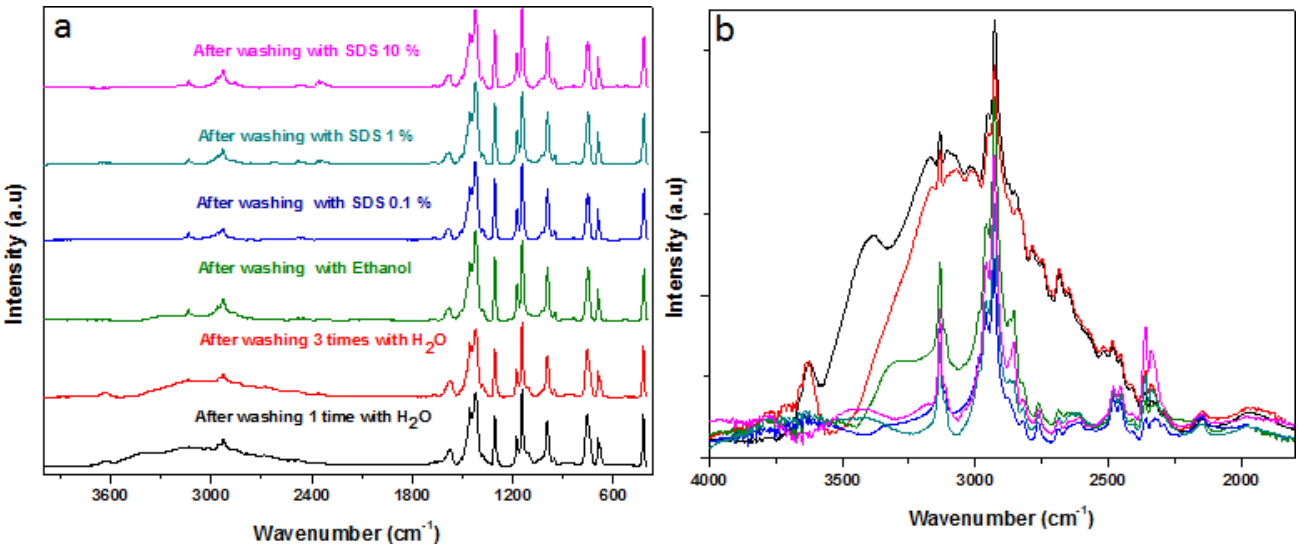

a) Pre-synthesized ZIF-8 subsequently exposed to CM-dextran. These samples were washed with H_2O one time (black), H_2O three times (red), ethanol (green), SDS 0.1 % (blue), SDS 1% (cyan) and SDS 10 % (magenta) b) Magnified spectra in the 4000-1800 cm^{-1}. The broad band between 3500 and 2500 cm^{-1} corresponds to OH groups from CM-dextran after washing with H_2O, EtOH and SDS. Washing with EtOH removed the majority of CM-dextran, so washing with SDS was considered unnecessary.

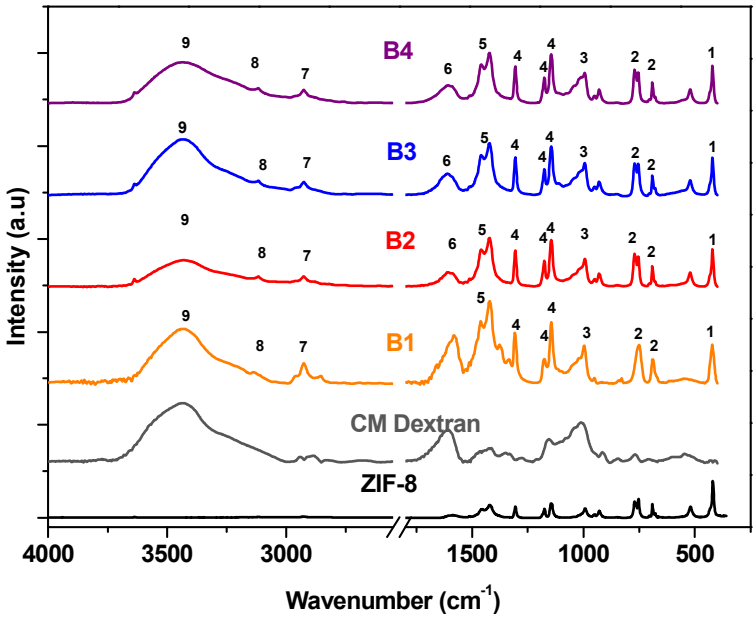

Figure S43. FTIR spectra of various CM-dextran@ZIF-8 B recipes (Zn^{2+}:2mIM = 1:3.47).

The assignment of the vibrational modes is reported in the table below.

Table of FTIR interpretation of CM-dextran B recipes

No	Characteristic Absorptions (cm^{-1})	Functional Group	References
1	421	Zn-N stretching	2
2	600-800	Out plane bending of the 2mIM ring	2 3
3	900-1350	In plane bending of the 2mIM ring	2 3
4	997	C-O stretching of CM-dextran	4
5	1420	Entire ring stretching of 2mIM	5
6	1608	COO^- of CM-dextran	6 7
7	2926	Aliphatic C-H stretching of 2mIM	5
8	3120	Aromatic C-H stretching of 2mIM	5
9	2850-3600	O-H stretching	8

Sample B4 prepared using FITC-tagged CM-dextran as biomimetic mineralization agent

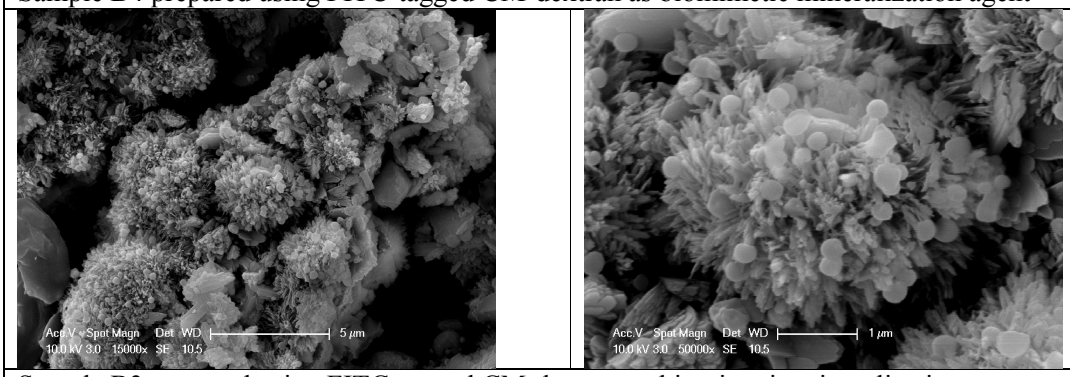

Sample B3 prepared using FITC-tagged CM-dextran as biomimetic mineralization agent

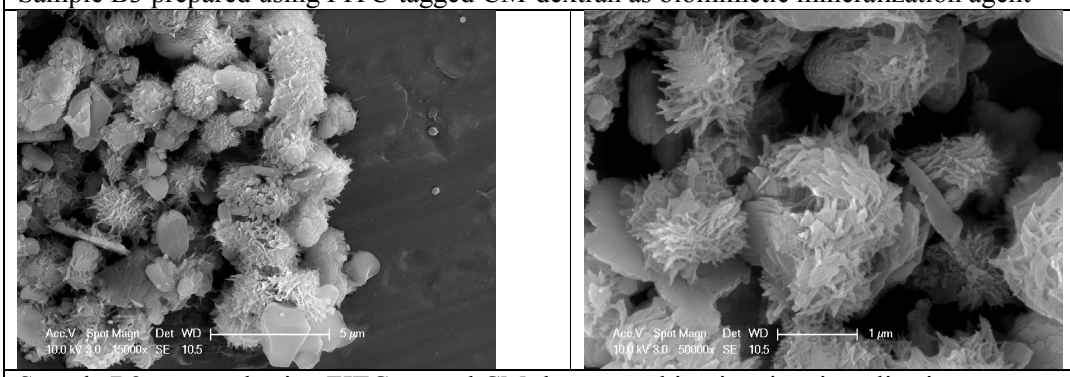

Sample B2 prepared using FITC-tagged CM-dextran as biomimetic mineralization agent

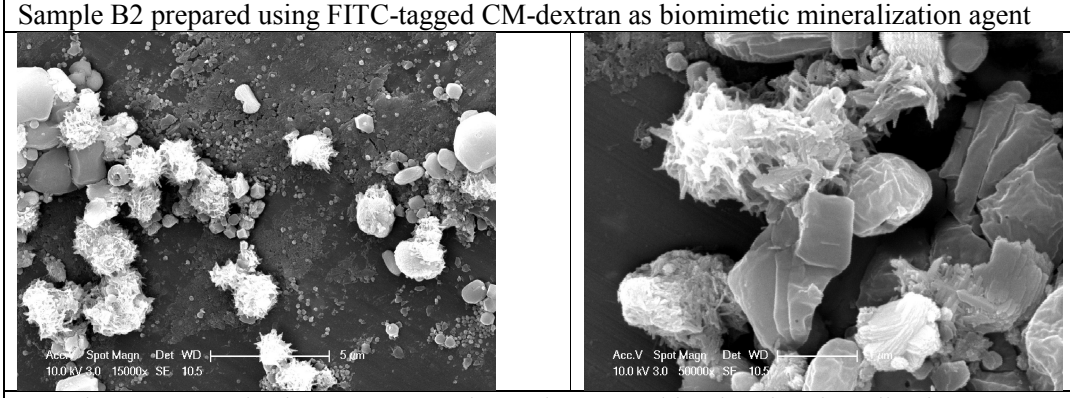

Sample B1 prepared using FITC-tagged CM-dextran as biomimetic mineralization agent

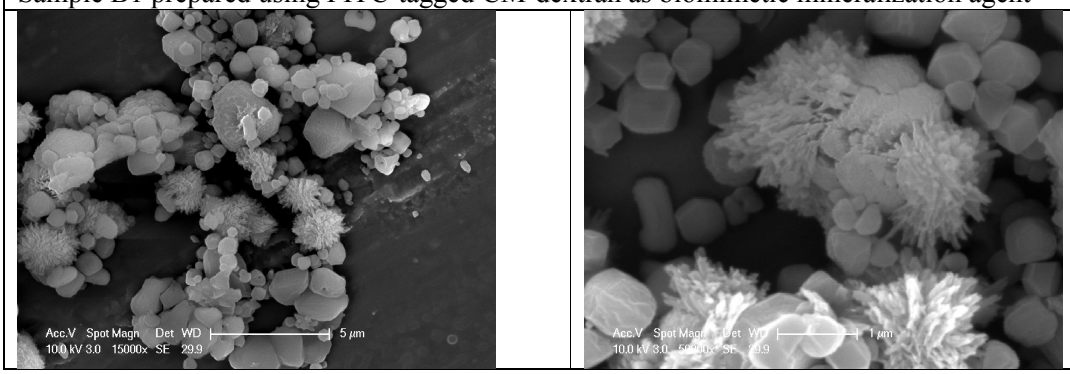

Figure S44. SEM image of ZIF-8 prepared using different concentrations of FITC-tagged CM-dextran: B1 = 0.18, B2 = 0.36, B3 = 0.72 and B4 = 1.44 mg mL^{-1}.

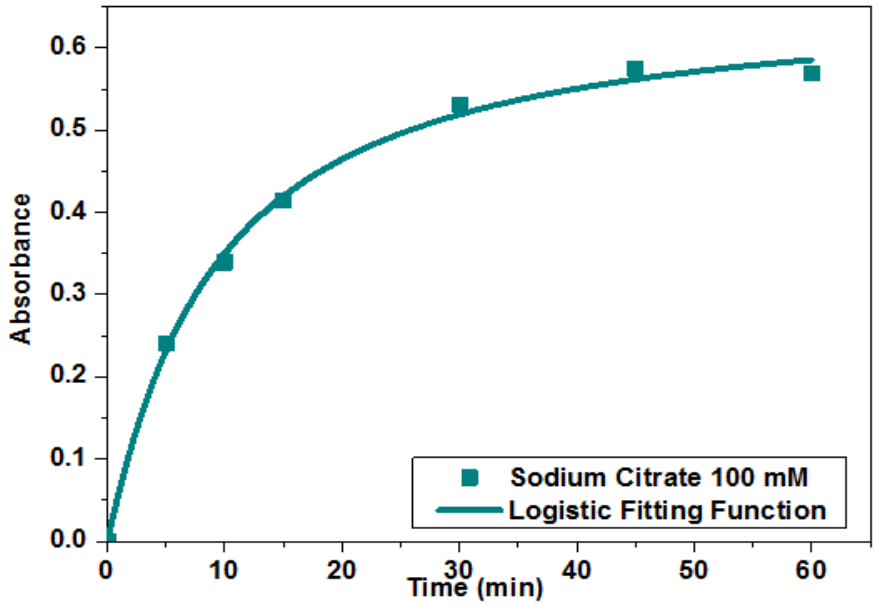

Figure S45. Release test of FITC-CM-dextran@ZIF-8 with 100 mM of sodium citrate (pH = 6).

$$Y = \frac{A2 + (A1 - A2)}{\left(1 + \left(\frac{x}{x0}\right)^{p}\right)}$$

Adj. R-Square 0.99375		
	Value	Standard Error
A1	0.00104	0.01655
A2	0.66336	0.05128
x0	9.02336	1.55683
p	1.06347	0.19551

The release test procedure of BF2 with sodium citrate was similar to release test with EDTA. Sample was mixed with sodium citrate solution 100 mM. The sample was vortex mixed for three second. At regular interval of 1 hour the mixture was centrifuge 1 min at 11337 rcf, then 1 mL of supernatant taken with micropipettes.

Monitoring the absorbance at 490 nm with time (please see figure above), we could prove that FITC-CM-Dextran can be released from FITC-CM-Dextran@ZIF-8 exposed to the sodium citrate solution. The experimental points can be fitted using a logistic fitting function.

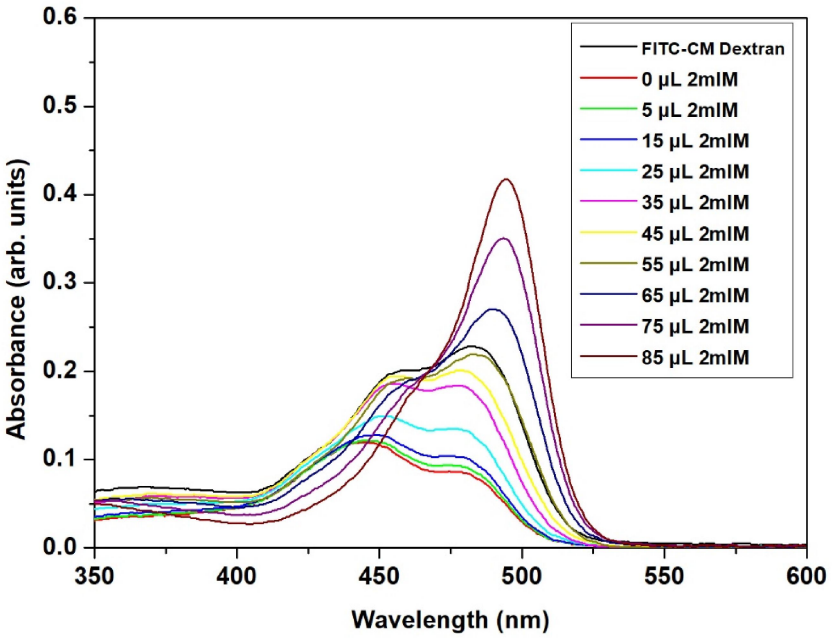

Figure S46. The UV-VIS absorbance of FITC-CM-dextran after adding EDTA, $Zn(OAc)_2.2H_2O$ and 2mIM.

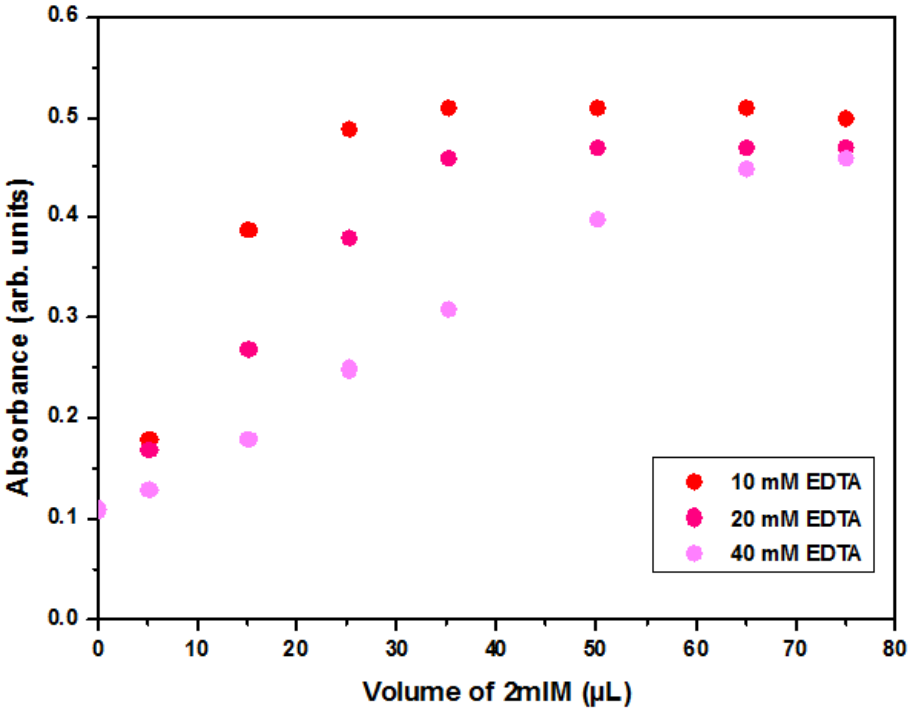

B3F Solution after release test	Volume Of Final Solution (µL)	Volume of 2 mIM (µL)	Absorbance		Correction Factor
			X	Y	F_{2mIM} = Y/X
10 mM EDTA	600	0	0.38		1.00
	600	12.5		0.38	
20 mM EDTA	600	0	0.22		1.76
	600	17.5		0.39	
40 mM EDTA	600	0	0.17		2.24
	600	32.5		0.38	

Figure S47. Correction Factor based on 2mIM was determined by measuring the absorbance intensity of FITC-CM-dextran at different concentrations of EDTA (10, 20, 40 mM) after adding 2mIM with different volumes.

The absorbance intensity of FITC-CM-dextran becomes constant after the addition of certain amount of 2mIM. Y is determined from absorbance intensity after adding the certain amount of 2mIM to the final solutions of release test with the different EDTA, meanwhile X is the absorbance intensity of the final solution after release tests with different concentration of EDTA. Correction factor based on 2mIM (F_{2mIM}) = Y/X.

References

1. Hodge, J. E. & Rist, C. E. The Amadori Rearrangement under New Conditions and its Significance for Non-enzymatic Browning Reactions. *J. Am. Chem. Soc.* **75,** 316–322 (1953).

2. Low, Z. X. *et al.* Crystal transformation in zeolitic-imidazolate framework. *Cryst. Growth Des.* **14,** 6589–6598 (2014).

3. Jian, M. *et al.* Water-based synthesis of zeolitic imidazolate framework-8 with high morphology level at room temperature. *RSC Adv.* **5,** 48433–48441 (2015).

4. Glišić, S., Nikolić, G., Cakić, M. & Trutić, N. Spectroscopic study of copper(II) complexes with carboxymethyl dextran and dextran sulfate. *Russ. J. Phys. Chem. A* **89,** 1254–1262 (2015).

5. Hu, Y., Kazemian, H., Rohani, S., Huang, Y. & Song, Y. In situ high pressure study of ZIF-8 by FTIR spectroscopy. *Chem. Commun.* **47,** 12694 (2011).

6. Repko, A., Nižňanský, D., Matulková, I., Kalbáč, M. & Vejpravová, J. Hydrothermal preparation of hydrophobic and hydrophilic nanoparticles of iron oxide and a modification with CM-dextran. *J. Nanoparticle Res.* **15,** (2013).

7. Sun, Y. X., Zhang, X. Z., Cheng, H., Cheng, S. X. & Zhuo, R. X. A low-toxic and efficient gene vector: Carboxymethyl dextran-graft- polyethylenimine. *J. Biomed. Mater. Res. - Part A* **84,** 1102–1110 (2008).

8. Heyn, A. N. J. The infrared absorption spectrum of dextran and its bound water. *Biopolymers* **13,** 475–506 (1974).

9. Rubinstein, M. & Colby, R. H. *Polymer physics*. *Polymer International* Oxford University Press, Oxford (2003).

10. Marszalek, P. E., Oberhauser, A. F., Pang, Y. P. & Fernandez, J. M. Polysaccharide elasticity governed by chair-boat transitions of the glucopyranose ring. *Nature* **396,** 661–664 (1998).

11. Rief, M., Oesterhelt, F., Heymann, B. & Gaub, H. E. Single Molecule Force Spectroscopy on Polysaccharides by Atomic Force Microscopy. *Science.* **275,** 1295–1298 (1997).

12. Shannon, R. D. Revised effective ionic radii and systematic studies of interatomic distances in halides and chalcogenides. *Acta Crystallogr. Sect. A* **32,** 751–767 (1976).

13. Simoes, M. C., Hughes, K. J., Ingham, D. B., Ma, L. & Pourkashanian, M. Estimation of the Thermochemical Radii and Ionic Volumes of Complex Ions. *Inorg. Chem.* **56,** 7566–7573 (2017).

14. Rayer, A. V., Sumon, K. Z., Jaffari, L. & Henni, A. Dissociation constants (pKa) of tertiary and cyclic amines: Structural and temperature dependences. *J. Chem. Eng. Data* **59,** 3805–3813 (2014).

15. Oliphant, T. E. Python for scientific computing. *Comput. Sci. Eng.* **9,** 10–20 (2007).

16. Wall, F. T. & Berkowitz, J. Numerical solution to the poisson-boltzmann equation for spherical polyelectrolyte molecules. *J. Chem. Phys.* **26,** 114–122 (1957).

17. Ohshima, H. & Kondo, T. Electrostatic double-layer interaction between two charged ion-penetrable spheres: An exactly solvable model. *J. Colloid Interface Sci.* **155,** 499–505 (1993).